Advances in
Geo-Energy Research

Vol. 19, No. 2, p. 146-165, 2026

Invited review

Advances in monitoring technologies for CO_2 geological storage: A review from the laboratory to field-scale applications

Yuhang Wang[1], Menglan Shi[1], Ning Wei[2], Aliakbar Hassanpouryouzband[3], Lanlan Jiang[1]*, Yongchen Song[1]*

[1]*Key Laboratory of Ocean Energy Utilization and Energy Conservation of Ministry of Education, Dalian University of Technology, Dalian 116024, P. R. China*

[2]*State Key Laboratory of Geomechanics and Geotechnical Engineering, Institute of Rock and Soil Mechanics, Chinese Academy of Sciences, Wuhan 430071, P. R. China*

[3]*School of Geosciences, University of Edinburgh, Grant Institute, Edinburgh EH9 3FE, United Kingdom*

Keywords:
CO_2 geological storage
CO_2 leakage
monitoring
optical fiber sensing technology

Cited as:
Wang, Y., Shi, M., Wei, N., Hassanpouryouzband, A., Jiang, L., Song, Y. Advances in monitoring technologies for CO_2 geological storage: A review from the laboratory to field-scale applications. Advances in Geo-Energy Research, 2026, 19(2): 146-165.
https://doi.org/10.46690/ager.2026.02.04

Abstract:
CO_2 geological storage is a pivotal technology for achieving the global targets of carbon peaking and carbon neutrality. However, the potential risks of CO_2 leakage to environmental safety and long-term storage efficacy are significant, thereby making the establishment of robust and reliable monitoring systems indispensable. This review systematically explores the potential leakage pathways and key monitoring parameters, including wellbore integrity, CO_2 plume migration, and caprock stability. In addition, the mechanisms and influencing factors associated with the three primary CO_2 leakage pathways are systematically summarized. This approach provides a critical assessment of the advantages, applicability and limitations of prevalent geophysical and geochemical monitoring methods. A special focus is placed on optical fiber sensing technology, whose research progress and application feasibility in laboratory settings are summarized in terms of monitoring targets, measurement accuracy and sensing range. Furthermore, this review highlights several global carbon capture and storage demonstration projects to illustrate the integration and performance of various monitoring technologies in practical engineering. To ensure the efficiency and safety of CO_2 geological storage in the future, it is necessary to develop advanced monitoring technologies, such as optical fiber sensing and promoting the integrated deployment of multi-modal monitoring systems. These efforts are considered essential for supporting the large-scale deployment of carbon capture, utilization and storage engineering, particularly in the context of China.

1. Introduction

1.1 Significance of monitoring CO_2 migration and leakage for geological storage

Global warming, primarily driven by increasing atmospheric concentrations of greenhouse gases, such as CO_2, poses a severe threat to the global climate system (Lu et al., 2025; Wang et al., 2025c; Zhu et al., 2025). Confronted with this challenge, CO_2 geological storage (CGS) has gained widespread attention as an effective mitigation technology for carbon peaking and carbon neutrality goals (Bashir et al., 2024; Baskaran et al., 2024; Bukar and Asif, 2024; Ren et

Yandy Scientific Press

*Corresponding author.
E-mail address: wangyuhang@mail.dlut.edu.cn (Y. Wang); 12310020@mail.dlut.edu.cn (M. Shi); nwei@whrsm.ac.cn (N. Wei); Hssnpr@ed.ac.uk (A. Hassanpouryouzband); lanlan@dlut.edu.cn (L. Jiang); songyc@dlut.edu.cn (Y. Song).
2207-9963
Received November 21, 2025; revised December 22, 2025; accepted January 13, 2026; available online January 16, 2026.

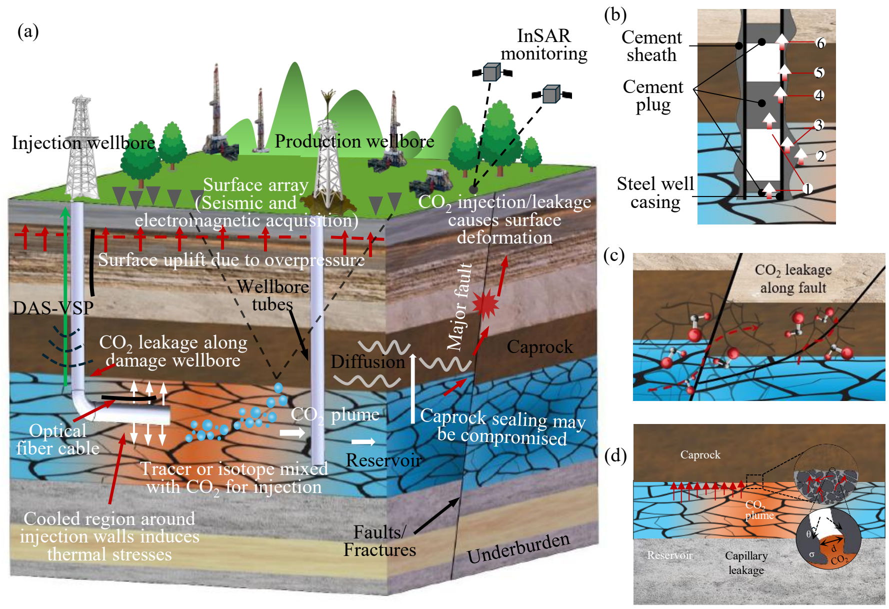

Fig. 1. Possible leakage pathways of CGS: (a) Geomechanical damage and CO_2 leakage, (b) wellbore leakage, (c) leakage via faults or fractures and (d) sealing leakage of the caprock, including diffusion leakage, seepage and fracture leakage.

al., 2025). It mainly includes depleted oil and gas reservoirs (Eigbe et al., 2023; Liu et al., 2023), deep saline aquifers (Li and Jiang, 2017), and unmined coal seams (Ding et al., 2025). Currently, 51 commercial carbon capture and storage (CCS) facilities are in operation worldwide, with a year CO_2 storage capacity of 41.6 million tonnes per annum (Mtpa). These are distributed across more than 50 countries and regions and have accumulated extensive practical experience (Global CCS Institute, 2024). The core focus of these projects lies in the selection of storage sites, storage capacity and long-term security. Since 1996, the Sleipner oil field project has successfully stored over 10 million tonnes of CO_2. However, several incidents of CO_2 leakage have been reported, highlighting several potential technical and geological risks. For instance, the Decatur Project in the United States experienced the leakage of approximately 8,000 tonnes of liquid CO_2 along with other fluids, primarily attributed to wellbore corrosion. Similarly, the Gorgon Project in Australia encountered leakage issues associated with insufficient caprock integrity. Therefore, it is vital to conduct further research on CO_2 leakage mechanisms, along with the development of monitoring strategies and integrity assessment methods for CO_2 storage systems.

As continuous CO_2 injection progresses in, the resulting increase in formation pressure may induce rock deformation or even fracture initiation, potentially leading to CO_2 leakage. Therefore, the real-time monitoring of critical parameters such as temperature, pressure and strain, as well as the tracking of fluid migration within the reservoir and caprock, is essential to ensure storage integrity and environmental safety. Consequently, a comprehensive monitoring program spanning subsurface, surface and atmospheric environments must be implemented across all stages: Pre-injection, during injection, and post-injection. This program is designed to verify the potential leakage and monitor CO_2 migration for the safety and long-term effectiveness of CGS.

1.2 Potential leakage pathways of CGS

The essential conditions for CO_2 leakage include: Sufficient CO_2 source, a driving force (such as pressure difference or buoyancy), and leakage pathways. As shown in Fig. 1, potential CO_2 leakage pathways are (1) through wellbore integrity damage and casing corrosion, (2) through the caprock, and (3) via pre-existing faults or fractures. On the one hand, formation heterogeneity and fracture networks may facilitate CO_2 migration into groundwater, lowering its pH, dissolving minerals and deteriorating water quality (Qafoku et al., 2017). Moreover, CO_2 leakage into near-surface soil may lead to soil acidification and alter its chemical composition. Seismic and volcanic activities, as well as changes in reservoir temperature and pressure, may also trigger CO_2 leakage (Kroeger et al., 2025). On the other hand, anthropogenic activities, such as oil-gas extraction and geological exploration, along with improper storage operations, can disturb the stability of geological storage. Excess injection pressure may further increase reservoir pressure, altering the physico-chemical properties of the caprock and ultimately resulting in CO_2 leakage. Besides, the escape of CO_2 into the atmosphere exacerbates the greenhouse effect. Therefore, our understanding of the leakage mechanisms through wellbore integrity, caprock sealing, and fractures or faults is important for tracking CO_2 migration in the long term.

Wellbore integrity is an important factor affecting the safety of long-term CGS. When the wellbore is not sealed properly, CO_2 may migrate upward. Furthermore, CO_2 leakage in abandoned wellbores is an another challenging issue (Celia et al., 2015). Generally, wellbore integrity can be divided into internal mechanical integrity and external mechanical integrity. The former involves leakage in the casing, tubing or packer, while the latter involves cement leakage outside the casing. The potential pathways for CO_2 leakage through the wellbore include: (1) Through the tubing (Chen et al., 2020; Deng et al., 2022), (2) around the packer (Zhang et al., 2023a), (3) across the casing (Ahammad and Azadbakht, 2025), (4) between the inside and outside of the casing and cement (Wolterbeek et al., 2013), (5) through the cement within the annulus (Lian et al., 2023), (6) via the cement-formation interface (Shi et al., 2025b), and (7) through cement plugs in abandoned wellbores (Peng et al., 2025). Due to the corrosive effect of CO_2 on tubes and casings, which causes diffusion leakage, the tubes and casings should be made of anti-corrosion materials. Cement is used to plug the casing to prevent CO_2 leakage from abandoned wellbores (Zhou et al., 2025).

Since CO_2 has low density, it will migrate upward under buoyancy forces, and pressure gradients from injection may also drive vertical and lateral movement along pre-existing faults or fractures in the formation. The main factors influencing CO_2 leakage along faults and fractures include fracture aperture, effective permeability, injection depth, injection rate, and reservoir heterogeneity (Yu et al., 2025). Consequently, although the effective caprock may be a thick, laterally extensive, low-permeability ($< 10^{-19}$ m^2), and undisturbed stratum, the presence of natural faults and fractures still pose a significant threat to caprock sealing.

Since the caprock plays an important role in underground CO_2 storage, it must possess certain characteristics. First, it needs to be impermeable to salt water and gas to prevent the upward migration of CO_2 (Saraf and Bera, 2021). Second it must have sufficient compressive and tensile strength to withstand the potential increase in pore pressure. Third, it must be buried at a sufficient depth to meet the requirements of temperature and pressure. CO_2 can migrate through caprock in three ways, including diffusion loss, capillary pressure, and the formation of faults/fractures due to excessive pressure. Among them, diffusion loss is mainly caused by the concentration difference leading to the CO_2 diffusion from formation to caprock. In this way, the structure of the caprock significantly affects the diffusion of CO_2. Once the pressure difference between the aqueous phase and the gas phase exceeds the maximum capillary pressure of the caprock, it will absorb CO_2. As CO_2 is less dense than the formation water under the pressure and temperature conditions of the target reservoir, the buoyancy of CO_2 will create a pressure difference on the sealing formation. During injection, the bottom pressure of the wellbore must be sufficiently high to enable effective CO_2 emplacement. As CO_2 dissolves in water, the accumulated fluid pressure will dissipate over time. However, to maintain integrity, the caprock must be capable of withstanding both short-term excess injection pressures and long-term buoyancy pressures. Ductility is an additional key property that enables the caprock to deform without developing fracture pathways for leakage.

When the wellbore leakage coefficient is $\leq 10^{-6}$, CO_2 is unlikely to escape through the wellbore. For instance, in the Shenhua Ordos CO_2 saline aquifer storage demonstration project, leakage over 1,000 years was estimated to be approximately 720 tonnes (Gan et al., 2024), which is below the 1% risk threshold proposed by the Intergovernmental Panel on Climate Change. However, when the leakage coefficient reaches $\geq 10^{-5}$, the risk of CO_2 leakage through the wellbore increases significantly. In addition, CO_2 stored in deep saline formations may migrate along faults due to pressure and concentration gradients, with studies indicating a leakage of about 3,000 tonnes over 100 years in highly permeable formations (Xia et al., 2017). In contrast, under the conditions of a homogeneous caprock and conventional gas reservoir characteristics, the complete leakage of CO_2 may take over 15×10^4 years (Zheng et al., 2010). Given the diverse mechanisms and potential hazards associated with different leakage pathways, ensuring storage safety requires precise site selection, effective pressure management, and long-term monitoring (Table 1). This review systematically examines the leakage mechanisms and influencing factors associated with wellbore integrity, fluid migration and caprock sealing across three leakage pathways in CGS. Subsequently, it highlights the urgent need for monitoring technologies, comparing the advantages and limitations of geophysical and geochemical methods for different research objectives. It then summarizes recent progress in laboratory-scale research and application feasibility of optical fibers, demonstrating the practical implementation of diverse monitoring techniques through example projects. Finally, it explores the application potential and future research directions of novel monitoring technologies, aiming to integrate multiple monitoring approaches to provide a sound theoretical foundation and scientific guidance for the efficient and safe storage of CO_2.

2. Existing research on the leakage monitoring mechanism

2.1 Wellbore integrity

2.1.1 Cement corrosion and material degradation mechanism

The injected CO_2 reacts with water to produce H_2CO_3 (carbonic acid), which corrodes the cement ring and casing in the wellbore. Meanwhile, high temperature and high pressure are major factors affecting wellbore integrity. Supercritical CO_2 ($scCO_2$) undergoes carbonation reactions with cement in the wellbore (Fig. 2(a)), with the relevant reaction equations are follows (Yan et al., 2021):

$$\begin{aligned} CO_2 + H_2O &\rightleftharpoons H_2CO_3 \rightleftharpoons H^+ + HCO_3{}^- \\ &\rightleftharpoons 2H^+ + CO_3{}^{2-} \end{aligned} \tag{1}$$

$$Ca(OH)_2 + CO_2 \longrightarrow CaCO_3\downarrow + H_2O \tag{2}$$

$$C{-}S{-}H + CO_2 \longrightarrow CaCO_3 + SiO_2 + H_2O \tag{3}$$

$$CO_2 + H_2O + CaCO_3 \longrightarrow Ca(HCO_3)_2 \tag{4}$$

where $Ca(OH)_2$ and calcium silicate hydrate (C-S-H) are the two primary hydration products of cement, and the ultimate products of this reaction are solid calcium carbonate ($CaCO_3$) and silica gel (SiO_2). The precipitation of $CaCO_3$ enhances the strength of the corrosion layer and reduces pore permeability (Qingyun et al., 2015; Qu et al., 2025). Furthermore, the dissolution of $scCO_2$ into formation water reduces the reser-

Table 1. Potential mechanisms of CO_2 leakage.

CO_2 leakage pathways	Probability/Risk level	Primary triggering mechanisms
Wellbore leakage	Most common/ Highest risk	Loss of wellbore integrity: • Cement degradation: Long-term aging, cement shrinkage leading to micro-annuli; • Casing corrosion: Acid corrosion due to CO_2 and impurities; • Seal failure: Damage to wellhead valves, packers or other components.
Fault/Fracture leakage	Low probability/ Serious consequences	Activation of geological features: • Pressure-induced activation: Reduced effective normal stress on faults due to injection pressure, leading to reactivation; • Induced seismicity: Fault slip triggering microseismic events.
Caprock leakage	Relatively low/ Challenging to monitor	Failure of caprock sealing mechanisms: • Capillary seal failure: Injection pressure exceeding capillary entry pressure of the rock; • Mechanical fracturing: Excessive injection pressure leading to hydraulic fracturing.

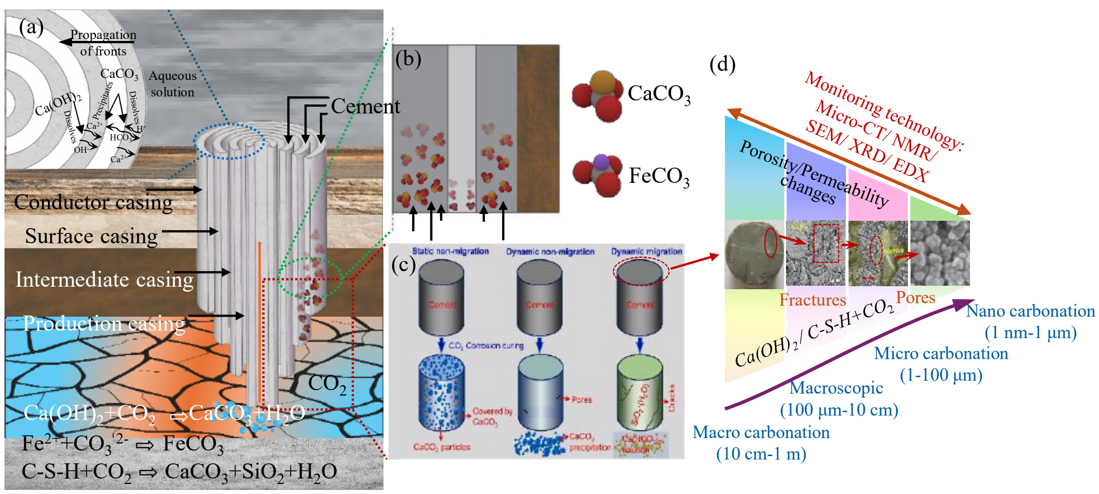

Fig. 2. Schematic diagram of the cement carbonation corrosion process: (a) Movement of $CaCO_3$ precipitates in cement, (b) precipitation and accumulation of $CaCO_3$ on the surface of cement, (c) CO_2 corroding cement process and (d) research scale of the cement carbonation process (Jung, 2013; Aparicio et al., 2022; Xue et al., 2022).

voir pH. Consequently, when CO_2(aq) and HCO_3^-(aq) are introduced into the reservoir, cement degradation may occur in injection, monitoring or abandoned wellbores. The carbonation process is directly related to the Gibbs free energy, with lower energy values corresponding to intensified carbonation. With the Ca/Si ratio decreases, the energy value increases (Batista et al., 2021). In addition, CO_2 reacts with Fe in the casing material to form siderite ($FeCO_3$) precipitates (Fig. 2(a)), thereby compromising wellbore integrity (Liu et al., 2024b). The relevant reaction can be expressed as (Nešić, 2007):

$$Fe^{2+}(aq) + CO_3{}^{2-}(aq) \longrightarrow FeCO_3(s) \tag{5}$$

The corrosion process of CO_2 on wellbore cement can be classified into three types: (1) Static non-migration process. In this case, CO_2 reacts with cement to form $CaCO_3$ particles, which in turn precipitate on the surface of the cement and occlude pre-existing pores (Fig. 2(b)); (2) Dynamic non-migration process. This refers to the corrosion-solidification mechanism in which CO_2 diffuses through pores and reacts with $Ca(OH)_2$ in cement to form $CaCO_3$. The latter precipitates within the pores without migrating to other regions; (3) Dynamic migration process. CO_2 not only reacts with cement to form $CaCO_3$ but also induces the dissolution of $SiO_2 \cdot H_2O$, producing soluble $Ca(HCO_3)_2$. This process can spread through pores to other regions, resulting in the development of fractures (Fig. 2(c)). Furthermore, according to experimental studies, the carbonation reaction between CO_2 and cement is usually studied by using technical means such as CT, NMR and SEM for multi-scale carbonation monitoring (Fig. 2(d)) (Cao et al., 2013; He et al., 2025), including macroscopic carbonation (10 cm-1 m), microfractures in cement (100 μm-10 cm), pore-scale carbonation (1-100 μm),

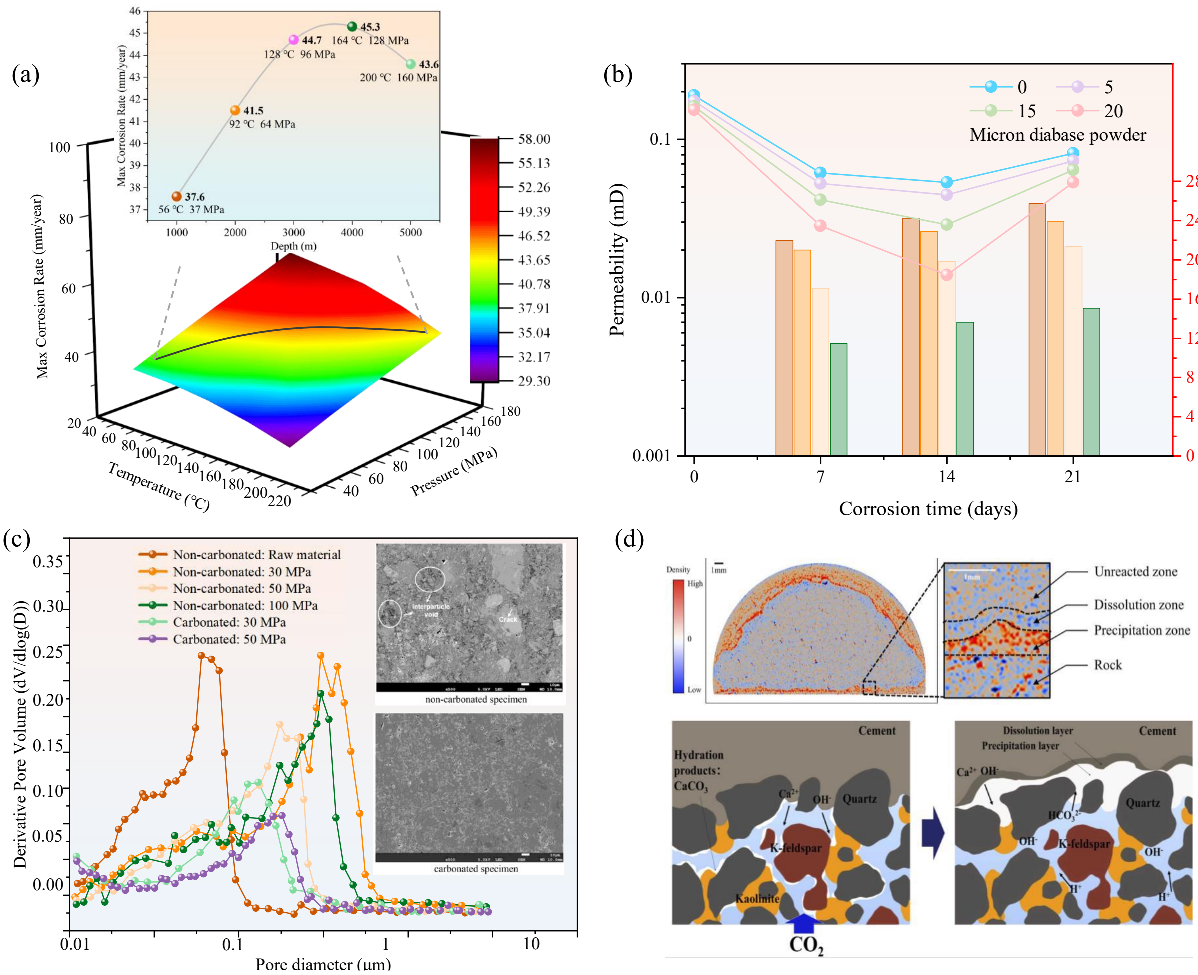

Fig. 3. Mechanisms governing the corrosion behavior and sealing performance of cement in CO_2 environments: (a) Effects of *in-situ* temperature-pressure conditions and wellbore depth on cement degradation (Peng et al., 2024), (b) influence of anti-corrosion materials on the corrosion permeability/porosity of cement (Zhong et al., 2024), (c) micromechanism of cement carbonation on wellbore integrity (Shao et al., 2025) and (d) schematic diagram of the CO_2 corrosion mechanism of cement (Shi et al., 2025a).

and nanoscale carbonation (1 nm-1 μm). Multi-scale experimental, numerical and theoretical studies are crucial for the quantitative assessment of wellbore integrity. Previous studies have shown that changes in parameters such as temperature, pressure, carbonation duration, and corrosive solution can alter the porosity and permeability of the cement structure, thereby affecting wellbore integrity and leading to unsafe CO_2 storage.

2.1.2 Factors affecting wellbore integrity

Temperature and pressure are among the most critical factors governing cement integrity and corrosion behavior in CO_2-rich environments. Carroll et al. (2017) analyzed the performance changes of Class H cement under simulated formation conditions (approximately 50 °C, 30 MPa) and found high temperature and high pressure enhanced cement hydration, resulting in a denser crystalline microstructure and improving resistance to carbonation. Compared with ambient temperature and low-pressure conditions, the carbonation depth was shallower and the structural damage less severe. Kutchko et al. (2007) found that cement exposed to high temperature and pressure develops a denser and more homogeneous $Ca(OH)_2$ microstructure and carbonation layer, leading to a reduction in corrosion depth. At varying pressures, the maximum corrosion rate of the wellbore decreases with increasing temperature, with the reduction becoming more pronounced at higher temperatures. Conversely, at varying temperatures, the maximum corrosion rate of the wellbore increases with rising pressure, and this increase becomes more significant at higher pressures. In addition, when the wellbore depth ranges from 1,000 to 5,000 m, the corrosion rate initially increases and then decreases with depth, due to the simultaneous rise in both temperature and pressure with increasing storage depth (Fig. 3(a)) (Peng et al., 2024; Song et al., 2024a). Both temperature and pressure affect CO_2 solubility (Pradhan et al., 2025). Specifically, the first dissociation constant of CO_2 increases with temperature up to 93 °C, but it decreases at temperatures above this threshold. From an electrochemical perspective, higher temperatures increase both the electrode polarization potential difference and the exchange current density. For low-carbon steel, in high-pressure environments

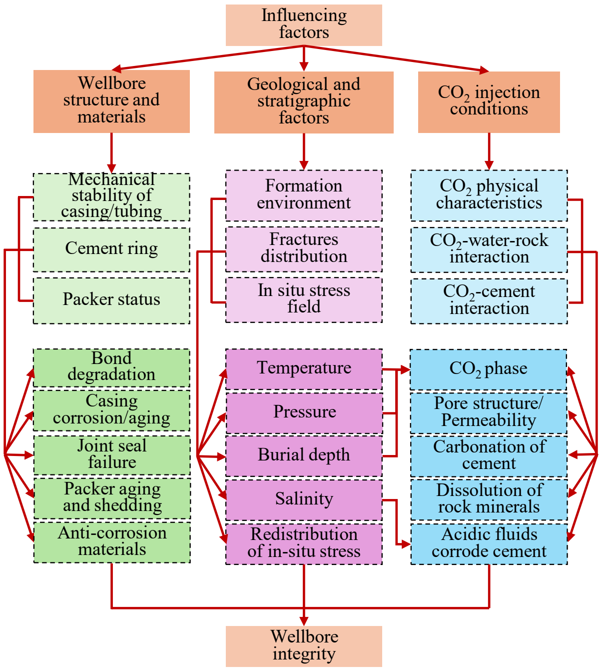

Fig. 4. Factors influencing wellbore integrity.

without the formation of a protective $FeCO_3$ film, the corrosion rate reaches 20 mm/year. However, if a stable $FeCO_3$ crystalline film forms, this may be significantly reduced to approximately 0.2 mm/year (Udebhulu et al., 2024).

In a $scCO_2$ environment (31.1 °C, 7.39 MPa), elevated temperature typically accelerates reaction kinetics and significantly affects the nucleation behavior of corrosion products on the steel surface. With increasing temperature, the nucleation rate of $FeCO_3$ markedly accelerates, facilitating the formation of denser and more protective corrosion scales. However, excessively high temperatures can lead to a looser $FeCO_3$ scale structure (Wang et al., 2024b). Therefore, temperature exerts a dual effect on corrosion processes in $scCO_2$ environments. Pressure plays a dominant role in the growth process of the corrosion scale layer. Under $scCO_2$ conditions, amorphous corrosion products initially form on the steel surface, which subsequently evolve into a dense inner $FeCO_3$ layer and finally result in the development of a relatively porous outer $FeCO_3$ layer. In contrast, in low-pressure CO_2 environments, the formation sequence of corrosion scale layers is reversed: A compact outer layer forms first, followed by a thicker but more porous inner layer. In general, the inner scale provides more effective protection for the substrate, especially under $scCO_2$ conditions (Wei et al., 2015).

Variations in the cement stress states and interfacial mechanical bonding strength are critical to wellbore integrity. Experimental results suggest that the degradation of mechanical bonding strength tends to be more pronounced at the cement-casing interface than at the cement-shale interface, making interfacial debonding a preferential pathway for CO_2 migration under adverse stress conditions (Bachu and Bennion, 2009; Wang et al., 2024a). Moreover, excessive tensile stress at the cement interface induces debonding and potential CO_2 leakage (Hwang et al., 2018). Besides, increasing pressure and burial depth lead to enhanced radial stress on the wellbore, as a greater overburden compression intensifies cement sheath confinement while reducing circumferential stress, which may shift from tensile to compressive regimes. However, Welch et al. (2020) found that the cement-casing interface is not a dominant CO_2 leakage pathway and that shear-driven failure poses limited risk. Wolterbeek et al. (2013) similarly concluded that the cement-casing bonding interface does not cause significant CO_2 leakage, whereas due to its limited healing ability, it may still become a potential leakage channel. This may be mitigated by carbonate precipitation, such as $CaCO_3$ from cement carbonation and $FeCO_3$ from casing corrosion, which can seal interfacial voids. Meanwhile, the injected low-temperature CO_2 redistributes the thermal and pressure fields of the wellbore-reservoir-caprock system, lowering temperature and increasing pressure, which may in turn induce micro-annuli, microfractures and fault reactivation, thereby compromising storage integrity.

Permeability and porosity are important properties for measuring the mutual flow of fluids in cement-sealed formations. The addition of anti-corrosion materials to cement generally results in low permeability (Sun et al., 2023). With an increasing addition amount of the anti-corrosion material diabase powder, the permeability gradually decreases, and as the corrosion proceeds, the permeability initially decreases and subsequently increases (Fig. 3(b)) (Zhong et al., 2024). However, Yan et al. (2023) observed a monotonic increase with exposure time. The decrease in permeability may result from pore clogging by $CaCO_3$ precipitates during early-stage corrosion. Moreover, the carbonation of compacted cementitious materials significantly optimizes pore structure. The carbonation reaction effectively reduces total porosity and refines the pore size distribution of both large (0.1-1 μm) and medium (0.01-0.1 μm) capillary pores. Before carbonation, large interparticle voids and visible fractures are observed, whereas after carbonation, calcium carbonate precipitation fill these voids and eliminate visible interparticle boundaries, producing a much denser structure (Fig. 3(c)) (Shao et al., 2025). In feldspar- and calcite-poor cores, carbonic acid promotes secondary mineral formation that blocks pores, while cement suppresses carbonate mineral dissolution but not clay dissolution (Fig. 3(d)) (Shi et al., 2025a). He et al. (2025) reported that direct corrosion with CO_2 increases the porosity of cement, while corrosion with CO_2-NaCl decreases the porosity of cement. In addition, the dissolution of $CaCO_3$ from carbonized cement may further enhance porosity (Marapira et al., 2025). Overall, permeability-porosity evolution is governed by the corrosive medium, exposure time and material modification, with microstructural processes such as clogging, dissolution-reprecipitation, and crystalline reorganization simultaneously controlling the long-term integrity of cement sealing systems.

The carbonation reaction is complex, and the variation mechanisms of cement permeability and porosity under different conditions remain poorly understood. Moreover, the failure mechanism of the cement-casing interface in a CO_2 environment still requires in-depth research. In fact, there are many factors affecting wellbore integrity (Fig. 4). Therefore, it is essential to conduct multi-scale and multi-factor coupled

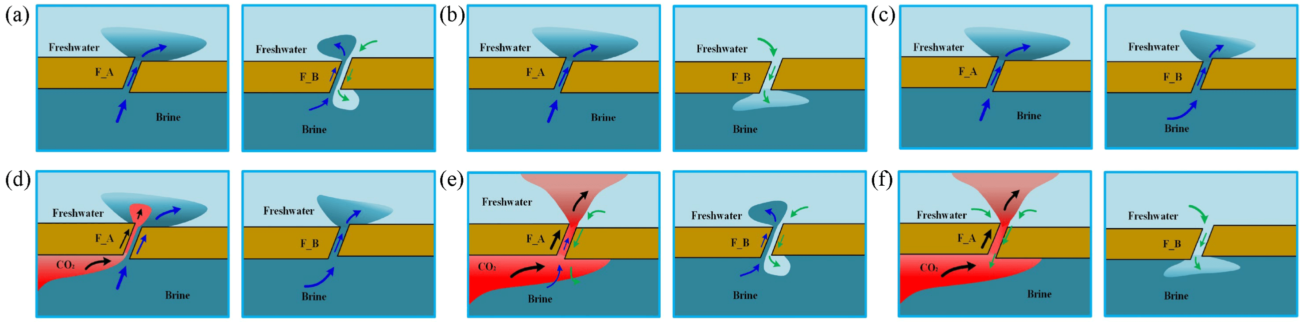

Fig. 5. CO_2, saltwater and freshwater in the saline aquifer migrate along the faults (Zhang et al., 2025): (a)-(f) represent Stages 1-6, respectively.

cement carbonation experiments to study the microstructure changes of cement under different conditions.

2.2 Fluid migration in CO_2 storage

Fluid migration within the geological formation is jointly controlled by multiple physical mechanisms. The migration modes include plume migration, molecular diffusion, convective dissolution, fingering flow, and channeling flow. When CO_2 is injected into saline aquifer, its density is lower than that of saltwater, therefore it flows upward within the reservoir. Under these conditions, convective fluid motion induces fingering flow. The formed "fingers" enhance mass transfer by increasing interfacial contact and the local concentration gradient. The data show that, compared with individual molecular diffusion, convective infiltration can significantly accelerate the dissolution rate of CO_2, thereby enhancing its dissolution and capturing efficiency and thus its long-term storage stability. Molecular diffusion is mainly driven by the CO_2 concentration gradient and is characterized by low transport rates and weak directionality. On a long timescale, although the diffusion rate is slow, it is of great significance for the risk assessment of CO_2 leakage, especially when there is uncertainty in the sealing performance of the fracture zone or the caprock. In addition, faults or fractures can act as preferential flow pathways, increasing the possibility of CO_2 leakage (Li et al., 2025). Therefore, understanding the fluid migration mechanisms is essential for the efficient storage and safe monitoring of CO_2 leakage.

2.2.1 Fluid plume migration mechanism

During the process of geological CO_2 storage, it is essential to conduct real-time monitoring of the injected CO_2 plume to ensure storage security. To this end, monitoring the dynamic reservoir variations and fluid migration has long been a core component in hydrocarbon reservoir development. When the vertical to horizontal permeability ratio is low, plume migration is dominated by lateral spreading, which may result in extensive horizontal movement. Conversely, when the vertical to horizontal permeability ratio is high, vertical migration is enhanced and CO_2 is more likely to accumulate beneath the caprock, driven by buoyancy and confined by caprock sealing capacity (Sohal et al., 2021; Yang and Okwen, 2024). Increasing the injection pressure significantly enhances CO_2 migration and displacement efficiency, thereby accelerating plume propagation and shortening leakage onset time, particularly in inclined and heterogeneous reservoirs (Jing et al., 2023; Qian et al., 2025). Pore-scale studies further indicated that higher pressure improves CO_2 sweep and storage efficiency in heterogeneous media, while in saline aquifers, CO_2 injection may further induce the coupled migration of brine and freshwater along faults, potentially increasing the leakage risk. Zhang et al. (2025) divided the fluid migration behavior along two faults into six stages (Fig. 5) under 11 MPa and 49 °C and summarized these six stages into four phenomena: (1) Severe brine overflow occurs prior to CO_2 leakage; (2) Freshwater reflux disappears in the second stage but reappears in the fifth stage; (3) The loss of brine and freshwater occurs simultaneously before the CO_2 leakage; (4) After CO_2 reaches the faults, brine and CO_2 leach upward together/escape, while freshwater flows downward. However, variations in the fault architecture, permeability, pressure, or salinity gradient may alter the sequence or intensity of these stages. Higher fault permeability accelerates overall fluid migration, resulting in a significant increase in the leakage of both CO_2 and freshwater.

2.2.2 Diffusion mechanism

The CO_2 diffusion in the saline aquifer through microfractures can be divided into two stages (Yu et al., 2025). The first stage is the dissolution of CO_2, whereas the second stage corresponds to aqueous diffusion at an approximately constant rate. During the dissolution stage, bubble morphology evolution enhances capillary trapping, reducing plume mobility and thereby mitigating leakage risks (Norouzi et al., 2021). In the second stage, CO_2 diffusion is controlled by fracture length and diffusion coefficients (Mehmani and Xu, 2024). As shown in Table S1, the diffusion coefficient of CO_2 in water/brine has been studied through simulation and/or experiments. Ramadhan et al. (2024) reported that under constant effective stress, elevated temperature increases the fluid density-to-viscosity ratio, enhancing fracture permeability and CO_2 penetration. However, under higher effective stress, mechanical closure suppresses plume mobility. Temperature and pressure exert substantial impacts on the diffusion coefficient, while significant discrepancies exist across studies, necessitating further work to clarify quantitative relationships among controlling

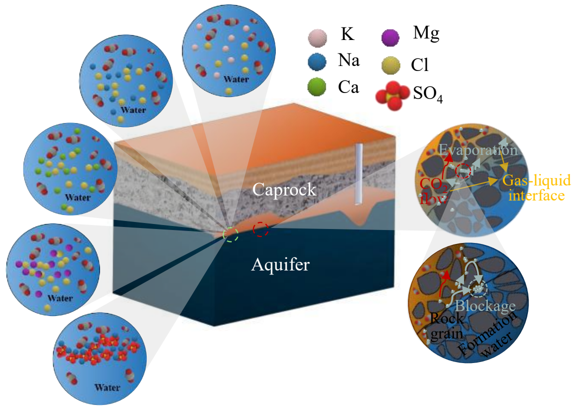

Fig. 6. Schematic diagram of the influence of different salt solutions on CO_2 transport and the mechanism of evaporation, salt precipitation and salt crystal migration clogging at the gas-liquid interface of CO_2 (Omrani et al., 2022; Sun et al., 2025).

factors for improved predictive accuracy.

From the investigations performed so far, it can be found that temperature, pressure and brine concentration will have a certain impact on the diffusion of CO_2 (Li et al., 2022a). Li et al. (2021) studied the effects of permeability, NaCl concentration, temperature, and pressure on the diffusion rate of CO_2. They found the diffusion coefficient increases with increasing permeability, pressure and temperature, but decreases with increasing NaCl concentration; moreover, the pressure effect gradually weakens and exhibits a nonlinear relationship with the CO_2 diffusion coefficient. Zhang et al. (2015) found that, under the relatively low temperature and low pressure conditions of 25-70 °C and 0.5-2.0 MPa, the CO_2 diffusion coefficient varies linearly with temperature and pressure. Zhang et al. (2023b) discovered that, within the reservoir depth range of 50-200 m, the diffusion coefficient of CO_2-brine shows a trend of increasing first and then decreasing with increasing depth.

Certain studies focused on the effects of ionic species in salt water on CO_2 diffusion. Omrani et al. (2022) investigated the effects of four salt solutions other than NaCl ($MgCl_2$, $CaCl_2$, KCl, and Na_2SO_4) on the diffusion coefficient of CO_2 at 50 °C and 10 MPa. They found that $CaCl_2$ had the greatest effect on the diffusion coefficient of CO_2, while KCl had the least influence. Wang et al. (2025a) further suggested that ion types (NaCl, $CaCl_2$, KCl) affect the CO_2 diffusion coefficient at lower pressures but have no effect on higher pressures. Because the solubility of CO_2 decreases with increasing ionic strength, and the presence of ions will block the passage of CO_2 molecules, inhibiting dynamic movement driven by the concentration gradient. The strong affinity between ions and water molecules leads to hydrated cluster formation, and larger hydrated clusters will further hinder the movement of CO_2 molecules. The tendency of CO_2 to form ionic aggregates is the strongest in a Na_2SO_4 solution, followed by $MgCl_2$, $CaCl_2$ and NaCl, while the tendency of CO_2 to form ionic aggregates is the weakest in a KCl solution (Fig. 6).

With ongoing CO_2 diffusion, evaporation-induced salt precipitation may occur at the CO_2-brine interface, reducing reservoir porosity. Salt crystallization, migration and pore-throat clogging represent the primary mechanisms of reservoir blockage, particularly near injection wellbores where salt precipitation is most likely. Therefore, further studies are required to quantify the coupled effects of pressure, temperature, salinity, and ionic species on CO_2 diffusion, to accurately predict salt precipitation and mitigate leakage risks. At present, predicting CO_2 plume migration under complex geological conditions remains highly challenging, due to factors such as reservoir heterogeneity and the unpredictability of fracture propagation. Furthermore, achieving the high-resolution, real-time, and comprehensive monitoring of CO_2 plumes remains limited by high costs, restricted spatial resolution, and the insufficient adaptability to complex geological settings. To enhance the safety and reliability of CO_2 geological storage, systematic experiments are needed to elucidate parameter-coupling mechanisms, alongside the development of more efficient, accurate and economically feasible CO_2 plume monitoring technologies.

2.3 Sealing of the caprock

2.3.1 Mechanism

When CO_2 is injected into the reservoir, capillary sealing occurs if the capillary entry pressure of the caprock exceeds the pore pressure of the reservoir, effectively preventing CO_2 from penetrating into the overlying formations. The combined effects of capillary pressure, adsorption resistance, and frictional resistance within the caprock govern the inhibition of CO_2 migration and escape. However, when reservoir pore pressure exceeds the breakthrough pressure of the caprock, preferential flow channels can form across the seal, allowing CO_2 to migrate and leak, thereby compromising the capillary sealing mechanism. Pore networks and microfractures constitute the primary pathways for CO_2 leakage through the caprock, and their abundance varies with lithology. Increased pore connectivity and fracture density significantly reduce sealing capacity, leading to an increased leakage risk (Chen et al., 2023).

Breakthrough pressure is a key parameter for characterizing caprock sealing, determined by the interplay of capillary forces, adsorption, and frictional resistance (Ma et al., 2020b). Capillary pressure depends on the caprock pore size, the interfacial tension (IFT) and the contact angle (CA) of the immiscible fluid (Chen et al., 2025a). The relevant expression is given as follows:

$$P_d = \frac{2\sigma\cos\theta}{r_0} + \lambda_1 H + \lambda_2 v \tag{6}$$

where P_d represents the breakthrough pressure, MPa; σ denotes IFT, N/m; θ denotes CA, °; r_0 stands for the minimum orifice throat radius, m; H denotes the thickness of caprock, m; v represents the movement velocity of CO_2 in the caprock, m/s; λ_1 denotes the adsorption resistance coefficient; λ_2 denotes the frictional resistance coefficient.

The most critical petrophysical factors for evaluating the sealing safety of the caprock are the wettability and IFT of the CO_2-brine-rock system. Table S2 summarizes the recent advances in caprock sealing safety monitoring. The

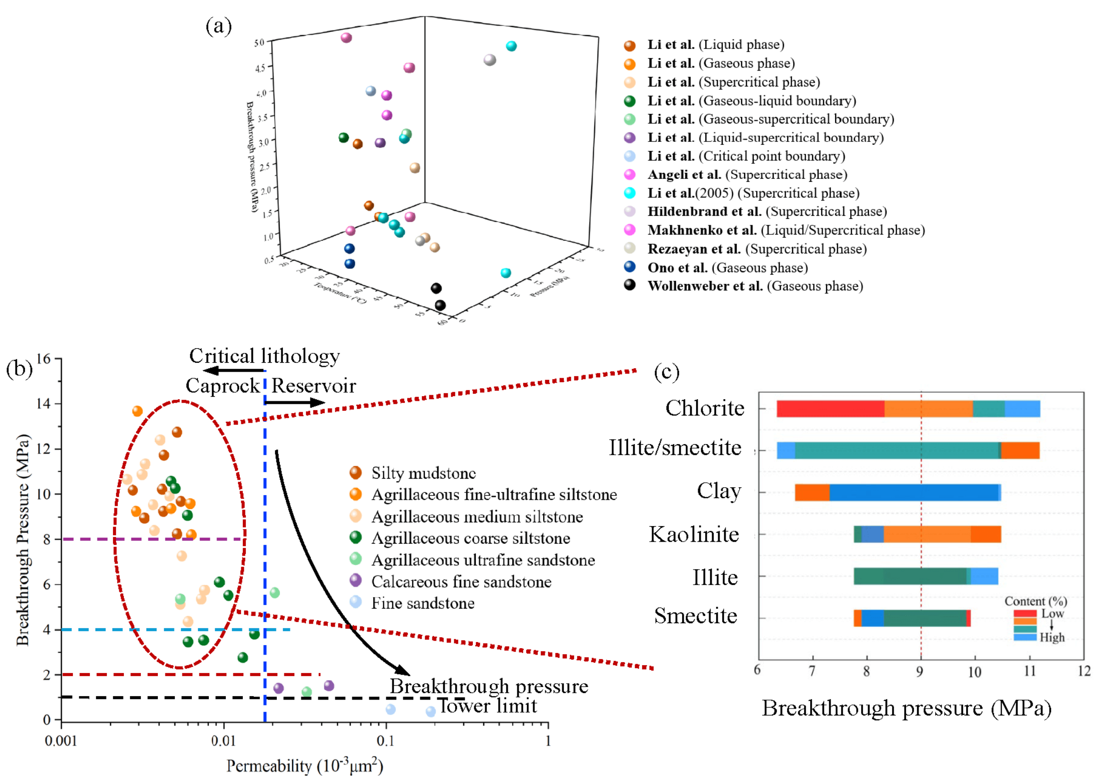

Fig. 7. Influence of different caprock lithologies: (a) Breakthrough pressure variations occurring with temperature and pressure (Hildenbrand et al., 2004; Li et al., 2005; Angeli et al., 2009; Wollenweber et al., 2010; Rezaeyan et al., 2015; Li et al., 2025), (b) breakthrough pressures corresponding to different lithologies and permeability caprock (Ma et al., 2020a) and (c) relationship between clay minerals and breakthrough pressure (Chen et al., 2024).

underground environment, including temperature, pressure, caprock thickness, brine concentration and brine composition, influence CA and IFT to varying degrees.

2.3.2 Factors affecting the sealing of caprock

Numerous studies have been conducted on the sealing and safety of CO_2-brine-caprock. The common caprock types include shale, sandstone, anhydrite and carbonate rocks (such as dolomite, calcite). Regarding breakthrough pressure, Song et al. (2024b) showed that it is inversely proportional to caprock permeability and increases nonlinearly with caprock thickness and depth. Wei et al. (2014) conducted experimental research on the CO_2 breakthrough pressure of argillaceous siltstone. The results showed that the breakthrough pressure increases with rising temperature and decreasing CO_2 pressure. Yao et al. (2025) noticed the breakthrough pressure decreased with increasing molar percentage of CO_2 in the gas mixture. The research figured out that there is no fixed relationship in the magnitude of the breakthrough pressure between different CO_2 phases (Fig. 7(a)). The breakthrough pressure relationship between different phases of CO_2 varies with changes in temperature and pressure. The order of breakthrough pressure of the caprock is as follows: Salt rock > mudstone > limestone > siltstone > argillaceous siltstone > volcanic rock > sandstone (Stavropoulou and Laloui, 2022). Meanwhile, the order of the influence of clay minerals on the breakthrough pressure is as follows: Chlorite > illite and montmorillonite > kaolinite > illite > chlorite in the montmorillonite mixed layer (Figs. 7(b) and 7(c)) (Chen et al., 2024). Higher clay content reduces pore size and increases breakthrough pressure, thereby improving sealing efficiency (Wang et al., 2025b). However, under low clay contents, smectite minerals undergo geochemical alteration from precipitation to dissolution-dominated behavior, drastically weakening self-sealing capacity (Jeon et al., 2018). Owing to their high surface area and hydrophilicity, clay minerals further enhance the capillary resistance of the aqueous phase, increasing the capillary pressure required for CO_2 breakthrough (Amann-Hildenbrand et al., 2013; Jeon et al., 2014).

The contact angle is a key parameter for quantifying the wettability of fluid on rock surfaces. Cheng et al. (2024) found the capillary sealing capacity of the caprock decreases by 7.14%-22.22% with the changing in the pore structure and wettability. Meanwhile, the increase in the porosity of small pore diameters (< 200 nm) and CA promotes a reduction in breakthrough pressure. The water wettability of shale decreases with increasing hydrophobic quartz or with decreasing hydrophilic carbonate and clay mineral contents, and the CA of shale decreases with increasing porosity and macropore volume (Yang and Okwen, 2024; Liu et al., 2026). Moreover, CA increases with increasing pressure but decreases with increasing temperature (Fig. 8(a)). IFT decreases with increasing pressure until reaching a stable value. However, with increasing temperature, IFT gradually decreases at a low-

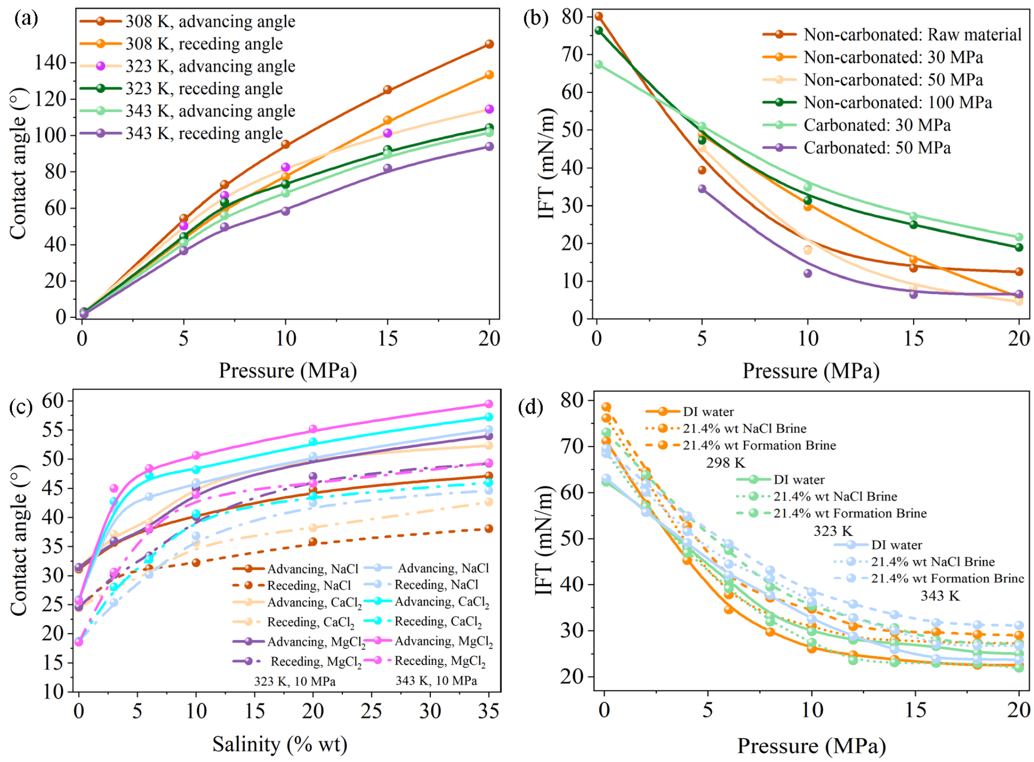

Fig. 8. Temperature, pressure, salinity, and saline type significantly affect CA and IFT: (a) CA variations with temperature and pressure (Arif et al., 2016), (b) IFT variations with temperature and pressure (Sarmadivaleh et al., 2015; Ali et al., 2022), (c) relationship between salinity, saline type and CA (Al-Yaseri et al., 2016) and (d) relationship between salinity, saline type and IFT (Mouallem et al., 2024).

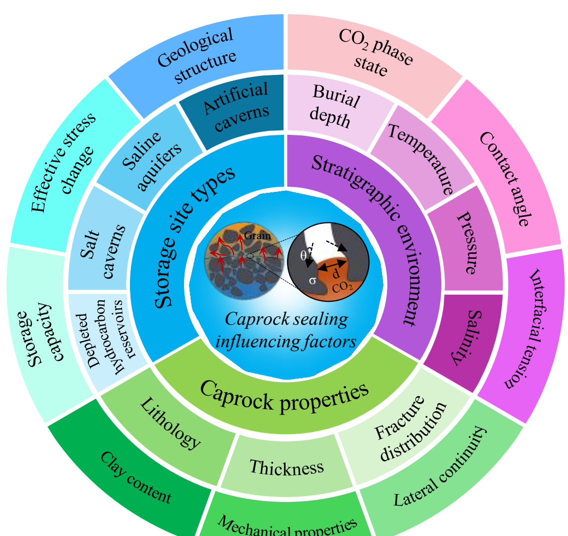

Fig. 9. Influencing factors of caprock sealing and geophysical safety.

er pressure and gradually increases at a higher pressure. IFT values vary among caprocks of different lithologies under identical temperature and pressure conditions (Fig. 8(b)). Moreover, the formation salinity influences capillary pressure by altering interfacial properties. Both IFT and CA exhibit positive linear correlations with salinity (Figs. 8(c) and 8(d)), which is attributed to enhanced electrostatic forces and ionic gradients at the gas-liquid-solid interface with increasing salinity. For different types of salt solutions, under the same thermophysical properties and saline concentration, CA and IFT rise with increasing ion valence (Chalbaud et al., 2006) as follows:

$$Cs^+ < Rb^+ < NH_4{}^+ < K^+ < Na^+ < Li^+ < Ca^{2+} < Mg^{2+} \quad (7)$$

The sealing and safety of the caprock depend on the reservoir type, the formation environment, and the caprock properties (Fig. 9). Wollenweber et al. (2010) found that the breakthrough pressure of N_2 was higher than that of CO_2, and the sealing efficiency of the caprock decreased with increasing test duration. IFT mainly affects the diffusion behavior of CO_2 in shale pores: When IFT is lower than 30 mN/m, CO_2 diffusion is significantly enhanced, especially in shale pores and fractures. Ellis et al. (2011) observed the fracture evolution in low-permeability carbonates by combining CT and SEM techniques. The preferential dissolution of calcite led to a significant increase in the surface roughness of fractures. In addition, the clay content in the caprock influences caprock sealing capacity. When the clay content in the rock is high enough, it may form a clay coating on the fracture wall, thereby preventing the dissolution of calcite, slowing down the fracture propagation and reducing the possibility of CO_2 leakage.

Among the primary pathways for CO_2 leakage, wellbores represent the pathway with the highest risk, as defects or degradation along the casing-cement-formation interface or within annular cement significantly compromise wellbore integrity. Leakage through pre-existing fractures or faults is generally less probable, though it may occur as short-term or episodic high-flux events. In caprock leakage, lithology and fracture distribution exert the strongest control. Most existing studies rely on laboratory-scale experiments or numerical simulations under simplified conditions, therefore, may not fully capture the coupled thermo-hydro-mechanical-chemical processes occurring in field-scale carbon capture, utilization and storage (CCUS) operations. Significant uncertainties remain in key parameters such as permeability evolution, interfacial bonding degradation, and CO_2 diffusion coefficients, leading to large variability in the model predictions. Therefore, further research is required to simulate realistic CO_2 storage conditions and to integrate high-resolution monitoring data with multiphysics models, thereby reducing uncertainties in CO_2 migration and leakage predictions.

3. Leakage monitoring technology

3.1 Geophysical/Geochemical methods

During CGS, the accurate tracking of CO_2 plume migration and the early identification of potential leakage pathways are essential for ensuring long-term storage security. The commonly used geophysical monitoring technologies include seismic methods, electrical resistivity, gravity monitoring, and InSAR remote sensing, which are effective for assessing wellbore integrity, plume migration and caprock sealing performance. Each technique offers their unique advantages for storage safety assessment but also exhibits their inherent limitations. In addition to geophysical approaches, geochemical methods provide effective means for leakage detection, such as isotopic tracers. Tracer-based monitoring, in particular, has been widely applied in petroleum, natural gas and geothermal systems owing to its low cost, high sensitivity and favorable cost-effectiveness, and has demonstrated considerable advantages in detecting CO_2 leakage from storage reservoirs.

Resistivity methods identify increases in resistivity associated with CO_2 displacing highly conductive brine, enabling the estimation of CO_2 saturation and distribution. This technique remains highly sensitive even at elevated CO_2 saturations, effectively compensating for the "blind spots" of seismic monitoring (Kim et al., 2011). It has been widely applied in onshore CO_2-EOR projects for inter-wellbore or single-wellbore monitoring, particularly when CO_2 saturation exceeds 20%, where resistivity responses outperform seismic velocity changes. Vertical seismic profile (VSP) data are also frequently used to calibrate surface seismic results. When combined with three-dimensional (3D) or four-dimensional (4D) seismic data, VSP measurements facilitate the analysis of the dynamic evolution of CO_2 plumes near the wellbore. In addition, commonly used tracers such as SF_6 and CH_4 can be detected at parts-per-million (ppm) concentrations and have been employed to assess the diffusion behavior of CO_2 in reservoirs, as well as to track the pathway and rates of CO_2 leakage in wellbore sampling. In an Australian CCS project, 300 kg of SF_6 was co-injected with 100,000 tonnes of CO_2, enabling the successful detection of the tracer signal at a monitoring wellbore 700 m from the injection site (Stalker et al., 2009).

Seismic monitoring is essential in tracking CO_2 migration within reservoirs by capturing changes in the elastic parameters (e.g., fluid saturation and pore pressure) caused by CO_2 injection (Padhi et al., 2014). The presence of CO_2 alters the seismic wave propagation characteristics, thereby affecting the P-wave velocity and attenuation; changes in the P-wave amplitude or propagation time can reflect variations in CO_2 saturation and pressure within the reservoir. Time-lapse (4D) seismic techniques have been widely applied to reservoir monitoring. Dong et al. (2025) found that an increase in porosity can alter the physical properties of rocks, resulting in increases in the longitudinal wave velocity and quality factor. The resistivity method can further dynamically detect the CO_2 injection and diffusion behavior, and it has a complementary relationship with the seismic method. Since the displacement of conductive brine by free-phase CO_2 causes a pronounced increase in resistivity, the technique is particularly effective in detecting early-stage plume evolution and plume boundary evolution. Gravity technology in wellbore has enabled the precise depiction of plume positions and CO_2 density estimation in multiple projects. When CO_2 migrates into shallow layers, it generates relatively large gravity anomalies (Zhang et al., 2024). Topham et al. (2020) demonstrated that measurable gravity signals (> 10 μGal) can be used to delineate the CO_2 plume position and predict the possible gravity changes in the reservoir during CO_2 injection and displacement. At the Sleipner site, the 3D fluid flow prediction was constrained and refined through the joint inversion of 4D seismic data, which improved the modeling of CO_2 plume migration in the Utsira sandstone reservoir. In addition, electrical resistivity tomography technology has been used to successfully monitor the CO_2 plume distribution in the reservoir (Schmidt-Hattenberger et al., 2014).

Caprock sealing remains the cornerstone of secure CO_2 storage, where any potential leakage must be rapidly detected and quantified using multi-technique approaches. InSAR technology evaluates caprock sealing performance by measuring surface deformation associated with subsurface pressure changes. It is particularly effective for regional-scale assessment of ground uplift or subsidence, as demonstrated in large-scale storage projects such as in In Salah (Algeria). The integration of InSAR with unmanned aerial vehicle remote sensing further enhances spatial resolution and enables the real-time identification of surface anomalies related to gas leakage. Moreover, when CO_2 migrates through the caprock and enters the shallow aquifer or the atmosphere, its isotopic composition will change due to mixing. By monitoring the variations in carbon-oxygen isotope ratios, trace amounts of CO_2 escape behavior can be revealed (Greenhouse, 2015). The rare gases He, Ar and Kr have been used as natural tracers to reveal the CO_2 dissolution behavior and displacement efficiency, as evidenced at the Cranfield and Otway sites (Linda et al., 2014).

3.2 Grating optical fiber monitoring

3.2.1 Fiber Bragg grating monitoring

To date, optical fiber sensing technology has been successfully applied in various monitoring fields such as petroleum and CO_2 storage. It can monitor parameters such as temperature, strain and acoustics, and has been be applied to soil and water conservation stability and geological disaster management (Eun et al., 2018). In CO_2-EOR operations, fiber Bragg grating (FBG) sensors have been deployed for monitoring processes at both the laboratory core-flooding scale and in deep to ultra-deep geological environments. Typically, these sensors are installed near the wellbore to capture subsurface fluid migration and saturation changes within the reservoir-caprock system.

FBG optical fiber sensors can monitor internal rock structural changes in real time with rapid response, along with the corresponding strain changes. Falcão et al. (2024) accurately monitored the strain changes of core samples caused by the variation of net confining pressure using FBG sensors in combination with NMR technology. They found that, as the confining pressure increases, the rock strain decreases linearly. Different phases of CO_2 can lead to differences in optical fiber monitoring responses. Studies have shown that the strain responses of the three different states after CO_2 injection into the sample increase with increasing pore pressure. The differences in the strain response times of the three fiber gratings, from largest to smallest, are liquid CO_2, scCO_2 and gaseous CO_2 (Fan et al., 2018). Tan et al. (2025) conducted research on the expansion process and strain behavior induced by seepage in the Longmaxi shale reservoir using FBG sensors, demonstrating the feasibility of applying optical fiber monitoring to the strain induced by seepage in reservoirs.

To more comprehensively and accurately study CO_2 leakage, the strain response can be better characterized by conducting comprehensive measurements of parameters, such as stress from both the axial and circumferential directions. It has been revealed that fault permeability increases sharply when effective stress falls below initial stress, indicating a heightened risk of CO_2 leakage, whereas sealing capacity is enhanced when effective stress exceeds the initial stress. Moreover, tensile strain is localized at fault centers, while compressive strain dominates peripheral regions, which is attributed to particle-end effects. During liquid CO_2 leakage, both pressure and temperature decrease sharply in the early stages before stabilizing, but this transient response was not observed in the case of gaseous CO_2 leakage (Xu et al., 2022). This phenomenon can be attributed to the latent heat associated with the phase transition of liquid CO_2 during leakage. When the leakage aperture is relatively small (about 0.2 mm), the phase change energy and pressure changes reach a dynamic equilibrium, thereby maintaining a constant pressure. When scCO_2 leaks along the faults, the response times of temperature and strain are approximately 1 times and 2.5 times longer than that of pressure. Although the feasibility of FBG-based monitoring for wellbore integrity, fluid migration and caprock sealing has been demonstrated, practical application still faces challenges related to deployment complexity and the comparatively high operational costs.

3.2.2 Distributed optical fiber monitoring

At present, in addition to the above-mentioned point-based optical fiber sensing technology, distributed optical fiber sensing technology is widely applied. Fig. S2 presents the application of distributed optical fiber sensing technology and the schematic diagrams of three types of scattered light (Liu et al., 2024a).

Distributed optical fiber strain sensing (DOFSS) can be employed to monitor wellbore conditions during CO_2 storage. In the event of compromised integrity of the injection or production casings, the leakage of fluids along preferential pathways induces perturbations in multiple physical fields within the wellbore, including acoustic, thermal, pressure, and electromagnetic fields. Consequently, measuring the changes in the distribution characteristics of physical fields is central to wellbore integrity monitoring. Permanent distributed optical fiber systems enable the accurate profiling of wellbore temperature and pressure, with deviations below 0.1%, facilitating the reconstruction of CO_2 injection profiles and the dynamic optimization of injection strategies (Deng et al., 2024). Distributed temperature sensing (DTS) has proven sensitive to thermal processes such as cement hydration, while distributed strain sensing (DSS) and coated fiber systems enable the detection of pressure-related and pH-related variations under high-temperature wellbore conditions, supporting cement integrity monitoring (Shumski et al., 2022; Amer et al., 2024). Li et al. (2022b) reviewed distributed acoustic sensing (DAS) in cement-casing integrity assessment. When DAS and DTS were used for multi-physics field collaborative monitoring, the results indicate that under high leakage rates and high differential pressures, the temperature and acoustic wave signals near the leakage point change significantly. However, low leakage conditions (≤ 0.5 L/min) produce weak signals, highlighting the necessity of hybrid monitoring strategies (Hu et al., 2025).

Owing to its high strain sensitivity (~ 0.5 $\mu\varepsilon$), DOFSS technology enables the real-time detection of rock deformation along the entire wellbore trajectory where optical fibers are installed (Zhang et al., 2019). It can deform in response to changes in minor pore pressure, and thus is widely used in surface deformation monitoring (Kishida et al., 2014). Meanwhile, some studies have found that the expansion behavior caused by CO_2 is more pronounced than that of other liquids (e.g., water and methane) (Heller and Zoback, 2014). Therefore, it is critical to monitor the CO_2 plume. Zhang et al. (2019) employed DOFSS and X-CT imaging techniques to monitor the fluid plume changes in sandstone rich in natural clay at the core scale, observing viscous fingering and wetting front displacement (Fig. 10(a)), and obtaining the rock strain changes caused by fluid injection at different times (Fig. 10(b)). These results demonstrate that DOFSS can be used to monitor the fluid plume changes and strain changes caused by fluid injection in sandstone reservoirs (Zhang and Xue, 2019). Based on the real-time monitoring method of DOFSS, Xu et al. (2024) investigated the changes in pore pressure, reservoir deformation and fluid plume migration process caused by fluid injection during CGS. By mapping

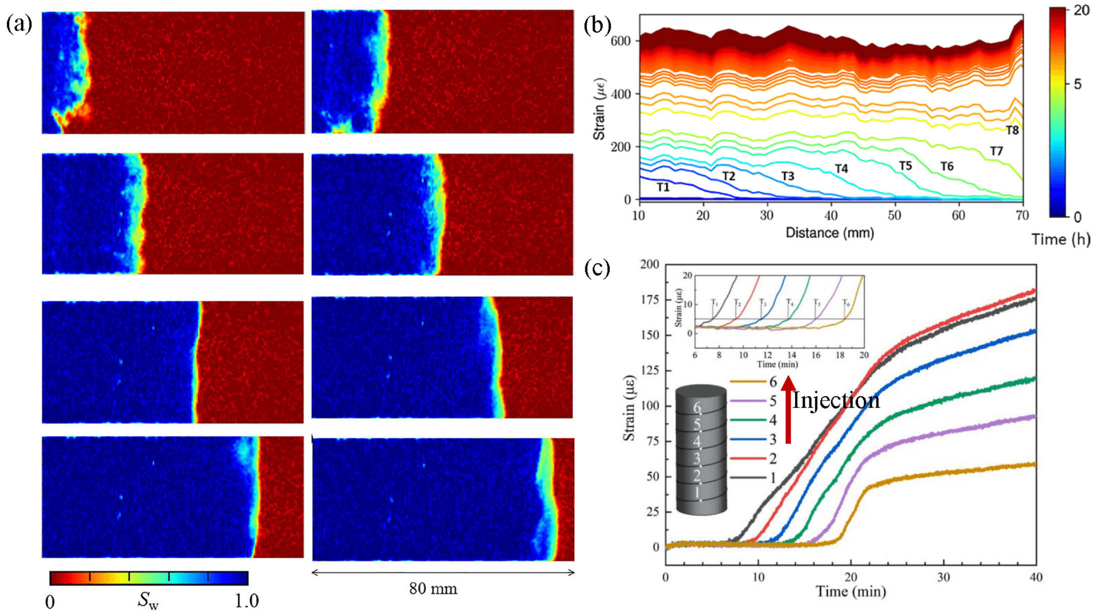

Fig. 10. Monitoring the front of fluid migration using distributed optical fiber technology: (a) Formation of the fluid plume front and water saturation (Zhang et al., 2019), (b) strain generated by the CO_2 plume process and (c) strain changes caused by fluid injection at different times (Xu et al., 2024) (Note: All the above-mentioned strain changes were monitored by DOFSS).

strain changes on rock surfaces, they tracked plume front location and migration velocity, demonstrating a progressive strain response from bottom to top during water injection (Fig. 10(c)). Collectively, these findings underscore the significant potential of optical fiber sensing technologies for the real-time monitoring of wellbore integrity, subsurface CO_2 migration, and fault leakage, thereby enhancing geomechanical modeling and contributing to long-term storage security.

Each monitoring technique for geological CO_2 storage inherently exhibits distinct advantages and limitations. From an economic perspective, the integration of optical fiber technology is particularly promising. Despite their benefits, optical fiber sensing systems face field-scale challenges related to long-term stability under harsh subsurface conditions and the interpretation of temperature, strain and acoustic signals under complex stress and in multiphase flow environments, particularly for low-rate leakage detection. Deployment in existing wellbores is further constrained by installation complexity and operational risks, while high installation and maintenance costs limit large-scale adoption. The lack of systematic cost-performance evaluations and long-term field demonstrations remains a key barrier to translating optical fiber monitoring from experimental studies to widespread CCUS application.

4. Typical monitoring projects at home and abroad

According to the latest report released by the Global CCS Institute, as of July 2024, a total of 628 CCUS projects worldwide were at various stages of development (Fig. 11). Compared with the previous year, the number of facilities had increased by 60.2%, while the overall CO_2 capture capacity had grown by 15.24%. In the following section, several representative CCS demonstration projects are reviewed and the monitoring technologies applied in these projects are analyzed.

4.1 Sleipner project

The Sleipner project in Norway pioneered the use of 4D seismic monitoring in combination with the world's first time-lapse gravity surveys to investigate a large-scale offshore CGS. It revealed the principle of CO_2 migration and accumulation underground during the CO_2 injection process. Observations demonstrated that CO_2 injection reduces the bulk density of the reservoir, thereby supporting safe storage evaluation and environmental risk assessment in complex geological settings. In Fig. 12, seismic difference maps acquired between 1994 and 2020 illustrate the spatial evolution of the injected CO_2 plume, within which a total of nine distinct high-amplitude anomalies can be identified. Following injection, increased CO_2 saturation, combined with the lower density of CO_2 relative to saline formation water, results in a reduced seismic wave velocity and decreased acoustic impedance in CO_2-saturated zones compared with brine-filled sandstones, and these changes are manifested as strong amplitude anomalies (yellow to red regions). Importantly, all anomalies remained confined to the Utsira reservoir, with no evidence of CO_2 migration into the overlying caprock. This indicates the absence of leakage and allows the detailed characterization of plume migration pathways along faults, folds, erosional surfaces, and depositional channels (Fig. 12). Since injection commenced in 1996, ten rounds of seismic monitoring have consistently verified the absence of detectable CO_2 leakage from the reservoir (White et al., 2018).

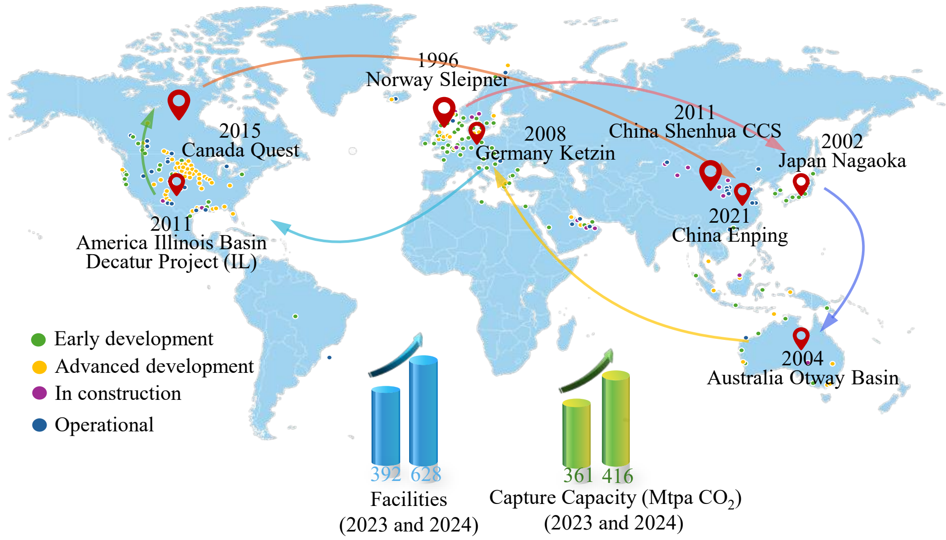

Fig. 11. Major global commercial CCUS monitoring projects.

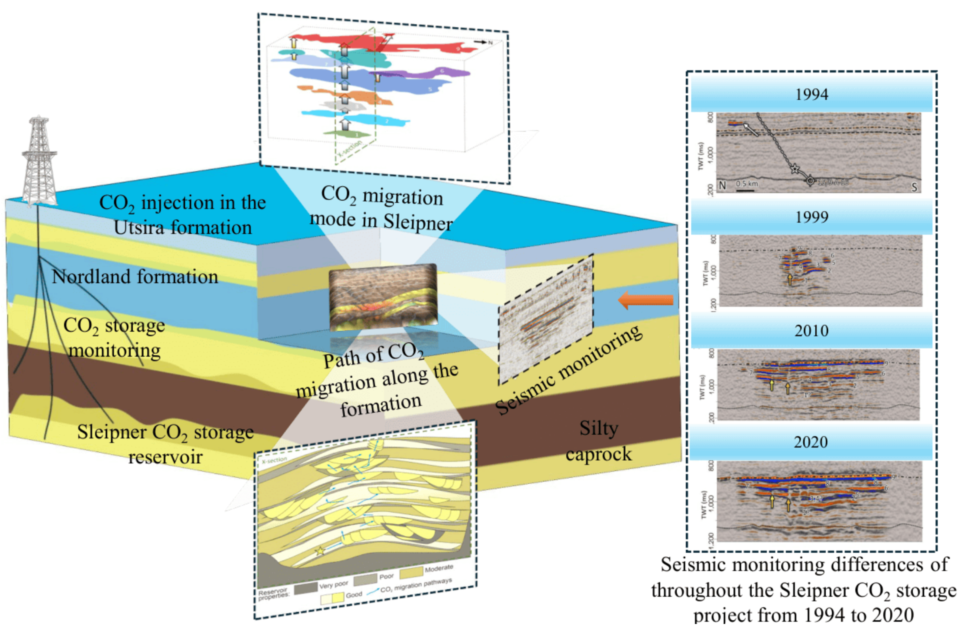

Fig. 12. Sleipner demonstration project for monitoring fluid migration (Furre et al., 2024).

4.2 Quest project

In 2015, the Quest CCS project in Canada commenced CO_2 injection into a deep saline aquifer at a depth of approximately 2,000 m (Fig. S3). Subsequently, a comprehensive measurement, monitoring and verification (MMV) framework was implemented, incorporating 4D seismic monitoring to evaluate plume containment and subsurface migration dynamics (Stephen et al., 2022). A range of monitoring techniques, including 3D and 2D seismic surveys, DAS, and multi-azimuth VSP, was deployed. Over the past decade, five seismic acquisition campaigns have been conducted. Time-lapse seismic data collected in 2016, 2017 and 2019 proved critical for accurately interpreting plume migration patterns (Fig. S3). Any leakage beyond the intended storage formation would have been indicated by anomalous seismic responses outside the reservoir. However, long-term monitoring has shown no evidence of leakage. Complementary tracer and isotopic analyses further validated the plume behavior, with $\delta^{13}C$ values of CO_2 varying by less than 2 ‰ over a 30-day period (Rock et al., 2014). These results demonstrate that integrated seismic monitoring and geochemical methods are effective at ensuring the safety of CO_2 storage in CCS projects.

4.3 Shenhua CCS demonstration project

The Shenhua CCS demonstration project in China represents the world's first full-chain CCS project integrated with coal-to-chemical processes (Fig. S4(a)). Preliminary investigations, including 3D seismic surveys, exploratory drilling, and numerical simulations indicated that the target deep saline aquifers possessed substantial CO_2 storage potential: A single wellbore was estimated to sustain an injection rate of 1.0×10^5 t/year for three years. The demonstration project established a comprehensive monitoring framework spanning subsurface, surface and atmospheric domains. Subsurface monitoring incorporated VSP, groundwater sampling and subsurface CO_2 flux measurements, all of which indicated no detectable breakthrough across the primary caprock (Fig. S4(b)) (Guo et al., 2015). In addition, downhole pressure and temperature logging was conducted *in situ* to assess reservoir conditions during injection. Meanwhile, the pH values of the aquifer overlying the caprock ranged from 7.19 to 7.59, while the groundwater temperature varied between 12.68 and 13.08 °C (Diao, 2017).

5. Prospects

Current research indicates that a monitoring framework for CO_2 storage has been preliminarily established and has shown promising feasibility. However, significant limitations, uncertainties and knowledge gaps remain. The prediction of CO_2 plume migration and leakage in complex geological settings is subject to substantial uncertainty, as heterogeneity, fracture networks and newly formed fractures can lead to discrepancies between monitoring observations and numerical simulation results. Geophysical methods, although suitable for large-scale imaging, are constrained by limited resolution and high costs, restricting their ability to detect small-scale leakage. Geochemical approaches, while highly sensitive, are susceptible to environmental disturbances and background noise. By contrast, optical fiber sensing technologies exhibit distinct advantages in terms of distributed, real-time, high-resolution monitoring of wellbore integrity, micro-fracture development, and dynamic pressure-temperature variations. Nonetheless, their long-term stability, deployment complexity, and low cost-effectiveness remain major barriers to large-scale implementation. Accordingly, future research on CGS monitoring should focus on the following key aspects:

1) With the continuous improvement of monitoring precision and data acquisition capabilities, future development is expected to focus on multi-physics, multi-scale and intelligent integrated monitoring systems. The fusion of geophysical, geochemical and optical fiber sensing techniques, coupled with machine learning and AI-driven inversion algorithms, will enable the creation of real-time, high-resolution, autonomous monitoring networks.
2) Although advanced optical fiber sensing systems show excellent potential, their high installation and maintenance costs continue to restrict large-scale implementation. Reducing system costs through material innovation, modular deployment and shared infrastructure will be essential for promoting commercial-scale CO_2 storage monitoring.
3) There is a pressing need for internationally unified standards and data-sharing frameworks governing CGS monitoring. Establishing unified international monitoring standards and open data-sharing frameworks will enhance the comparability of results, facilitate cross-project collaboration, and support transparent, long-term MMV mechanisms under global carbon neutrality initiatives.
4) Future monitoring systems should be designed that can endure harsh subsurface environments and maintain stability for decades. By integrating cloud-based data platforms and digital twin technologies, CO_2 storage sites can be managed through predictive simulations, risk visualization, and real-time anomaly alerts, enabling proactive responses to potential leakage or geomechanical instability issues.

6. Conclusions

CGS is a key technology for large-scale carbon mitigation. This review summarizes recent advances in leakage mechanisms and monitoring strategies, focusing on wellbore integrity, fluid migration, and caprock sealing. While geophysical and geochemical methods provide valuable large-scale and indirect information, they are often constrained by insufficient spatial resolution, real-time capability, and low cost-effectiveness. Optical fiber sensing technologies offer high-resolution, real-time, long-term monitoring, and a single permanently installed fiber can enable distributed, multi-parameter measurements over decades, significantly reducing repeated logging, wellbore interventions, and overall life-cycle costs. Integrated with geophysical and geochemical approaches, optical fiber sensing enhances multi-source data fusion and improves risk assessment capabilities. Future efforts should prioritize hybrid monitoring frameworks that combine advanced sensing, AI-based analysis, and standardized MMV protocols to ensure reliable, scalable and economically feasible CGS.

Acknowledgements

This study was supported by the National Key Research and Development Program of China for Young Scientists (No. 2023YFB4104100) and the National Science and Technology Major Project in China (No. 2024ZD1406604). The study was also supported by the Unveiling and Commanding Foundation of Liaoning Province (No. 2023JH1/10400003), and the Shenzhen Science and Technology Program (No. JCYJ20220818095605012). Meanwhile, this work was also supported by the Young Changjiang Scholars Programme of China.

Conflicts of interest

The authors declare no competing interest.

References

Ahammad, F., Azadbakht, S. A comprehensive review of factors affecting wellbore integrity in CO_2 injection wells. Energy Geoscience, 2025, 6(2): 100401.

Ali, M., Pan, B., Yekeen, N., et al. Assessment of wettability and rock-fluid interfacial tension of caprock: Implications for hydrogen and carbon dioxide geo-storage. International Journal of Hydrogen Energy, 2022, 47(30): 14104-14120.

Al-Yaseri, A. Z., Lebedev, M., Barifcani, A., et al. Receding and advancing (CO_2 + brine + quartz) contact angles as a function of pressure, temperature, surface roughness, salt type and salinity. The Journal of Chemical Thermodynamics, 2016, 93: 416-423.

Amann-Hildenbrand, A., Bertier, P., Busch, A., et al. Experimental investigation of the sealing capacity of generic clay-rich caprocks. International Journal of Greenhouse Gas Control, 2013, 19: 620-641.

Amer, R., Xue, Z., Hashimoto, T., et al. Distributed fiber optic temperature and strain sensing in cementing and water injection: Insights to well integrity monitoring and multisensing optical fiber cable design. Gas Science and Engineering, 2024, 130: 205430.

Angeli, M., Soldal, M., Skurtveit, E., et al. Experimental percolation of supercritical CO_2 through a caprock. Energy Procedia, 2009, 1(1): 3351-3358.

Aparicio, P., Martín, D., Baya-Arenas, R., et al. Behaviour of concrete and cement in carbon dioxide sequestration by mineral carbonation processes. Boletín de la Sociedad Española de Cerámica y Vidrio, 2022, 61(3): 220-228.

Arif, M., Al-Yaseri, A. Z., Barifcani, A., et al. Impact of pressure and temperature on CO_2-brine-mica contact angles and CO_2-brine interfacial tension: Implications for carbon geo-sequestration. Journal of Colloid and Interface Science, 2016, 462: 208-215.

Bachu, S., Bennion, D. B. Experimental assessment of brine and/or CO_2 leakage through well cements at reservoir conditions. International Journal of Greenhouse Gas Control, 2009, 3(4): 494-501.

Bashir, A., Ali, M., Patil, S., et al. Comprehensive review of CO_2 geological storage: Exploring principles, mechanisms, and prospects. Earth-Science Reviews, 2024, 249: 104672.

Baskaran, D., Saravanan, P., Nagarajan, L., et al. An overview of technologies for capturing, storing, and utilizing carbon dioxide: Technology readiness, large-scale demonstration, and cost. Chemical Engineering Journal, 2024, 491: 151998.

Batista, G. d. S., Schemmer, L. B., Siqueira, T. d. A., et al. Chemical resistance and mechanical properties of nanosilica addition in oil well cement. Journal of Petroleum Science and Engineering, 2021, 196: 107742.

Bukar, A. M., Asif, M. Technology readiness level assessment of carbon capture and storage technologies. Renewable and Sustainable Energy Reviews, 2024, 200: 114578.

Cao, P., Karpyn, Z. T., Li, L. Dynamic alterations in wellbore cement integrity due to geochemical reactions in CO_2-rich environments. Water Resources Research, 2013, 49(7): 4465-4475.

Carroll, S. A., Iyer, J., Walsh, S. D. C. Influence of chemical, mechanical, and transport processes on wellbore leakage from geologic CO_2 storage reservoirs. Accounts of Chemical Research, 2017, 50(8): 1829-1837.

Celia, M. A., Bachu, S., Nordbotten, J. M., et al. Status of CO_2 storage in deep saline aquifers with emphasis on modeling approaches and practical simulations. Water Resources Research, 2015, 51(9): 6846-6892.

Chalbaud, C. A., Robin, M., Egermann, P. Interfacial tension data and correlations of brine-CO_2 systems under reservoir conditions. Paper SPE 102918 Presented at The SPE Annual Technical Conference and Exhibition, San Antonio, Texas, USA, 24-27 September, 2006.

Chen, B., Li, Q., Tan, Y., et al. Experimental measurements and characterization models of caprock breakthrough pressure for CO_2 geological storage. Earth-Science Reviews, 2024, 252: 104732.

Chen, B., Li, Q., Tan, Y. Caprock sealing for geologic CO_2 storage: Research advances, challenges and prospects. Journal of Rock Mechanics and Geotechnical Engineering, 2025a, 18(1): 335-363.

Chen, B., Wang, R., Li, Q., et al. Status and advances of research on caprock sealing properties of CO_2 geological storage. Geological Journal of China Universities, 2023, 29(1): 85-99. (in Chinese)

Chen, S., Wang, H., Wang, Y., et al. Residual mechanical strength evaluation of corroded tubing in cryogenic carbon dioxide injection wellbore. Journal of Petroleum Science and Engineering, 2020, 193: 107398.

Cheng, Q., Tang, J., Liu, Y., et al. Capillary sealing capability alteration of shale caprock induced by CO_2-brine-rock interaction: Implication for CO_2 geological storage. Geoenergy Science and Engineering, 2024, 241: 213149.

Chen, S., You, H., Xu, J., et al. Leakage monitoring of carbon dioxide injection well string using distributed optical fiber sensor. Petroleum Research, 2025b, 10(1): 166-177.

Deng, C., Cao, B., Dang, L., et al. Application of permanent optical fiber monitoring technology in the first offshore carbon reinjection well. Petrochemical Industry Technology, 2024, 31(1): 68-70+61. (in Chinese)

Deng, K., Zhou, N., Lin, Y., et al. Study on residual strength and life prediction of corroded tubing based on thermal-mechanical coupling XFEM. Ocean Engineering, 2022, 255: 111450.

Diao, Y. Study on the reservoir characterization and CO_2 migration underground in the shenhua CCS demonstration project site. Beijing, China University of Mining & Technology, 2017. (in Chinese)

Ding, Y., Li, B., Li, J., et al. Characteristics of CO_2 adsorption influenced by coal pore structure-temperature interaction, including its implications for geological storage. Chemical Engineering Journal, 2025, 518: 164626.

Dong, Y., Shen, Y., Guo, K., et al. Characterization of petrophysical and seismic properties for CO_2 storage with sensitivity analysis. Petroleum Science, 2025, 22(1): 193-209.

Eigbe, P. A., Ajayi, O. O., Olakoyejo, O. T., et al. A general review of CO_2 sequestration in underground geological formations and assessment of depleted hydrocarbon reservoirs in the Niger Delta. Applied Energy, 2023, 350: 121723.

Ellis, B. R., Bromhal, G. S., McIntyre, D. L., et al. Changes in caprock integrity due to vertical migration of CO_2-enriched brine. Energy Procedia, 2011, 4: 5327-5334.

Eun, J. H., Huitaek, Y., Hwan, J. S., et al. A review on optical fiber sensors for environmental monitoring. International Journal of Precision Engineering and Manufacturing-Green Technology, 2018, 5(1): 173-191.
Falcão, B. D. S., Esteban, L., Giwelli, A., et al. Rock structural changes monitored by fibre bragg grating sensors and nuclear magnetic resonance during static and dynamic carbonated brine core flooding experiments. Fuel, 2024, 367: 131437.
Fan, C., Li, Q., Li, X., et al. Dynamic optical fiber monitoring of water-saturated sandstone during supercritical CO_2 injection at different sequestration pressures. Paper Presented at Proceedings of the 8th International Congress on Environmental Geotechnics Volume 3, Singapore, 28 October-1 November, 2018.
Furre, A.-K., Warchoł, M. J., Alnes, H., et al. Sleipner 26 years: How well-established subsurface monitoring work processes have contributed to successful offshore CO_2 injection. Geoenergy, 2024, 2(1): 15.
Gan, M., Lei, H., Zhang, L., et al. Quantitative evaluation method of wellbore leakage risk of CO_2 geological storage project based on numerical simulation. Advanced Engineering Sciences, 2024, 56(1): 195-205. (in Chinese)
Global CCS Institute. Global status of CCS 2024. Global CCS Institute, 2024.
Greenhouse, G. C. Assessing the usefulness of the isotopic composition of CO_2 for leakage monitoring at CO_2 storage sites: A review. Chemicals & Chemistry, 2015, 37: 46-60.
Guo, J., Wen, D., Zhang, S., et al. Potential evaluation and demonstration project of CO_2 geological storage in China. Geological Survey of China, 2015, 2(4): 36-46. (in Chinese)
Heller, R., Zoback, M. Adsorption of methane and carbon dioxide on gas shale and pure mineral samples. Journal of Unconventional Oil and Gas Resources, 2014, 8: 14-24.
He, Y., Song, L., Ranjith, P. G., et al. Evolution of resistivity and permeability of wellbore cement after corrosion by supercritical CO_2 in geological CO_2 storage conditions. Construction and Building Materials, 2025, 473: 141015.
Hildenbrand, A., Schlömer, S., Krooss, B. M., et al. Gas breakthrough experiments on pelitic rocks: Comparative study with N_2, CO_2 and CH_4. Geofluids, 2004, 4(1): 61-80.
Hu, H., Meng, G., Chen, L., et al. Leakage diagnosis method of injection-production string in underground gas storage wellbore based on cooperative monitoring of multi-physical fields. Measurement, 2025, 255: 118092.
Hwang, J., Ahmed, R., Tale, S., et al. Shear bond strength of oil well cement in carbonic acid environment. Journal of CO_2 Utilization, 2018, 27: 60-72.
Jeon, P. R., Choi, J., Yun, T. S., et al. Sorption equilibrium and kinetics of CO_2 on clay minerals from subcritical to supercritical conditions: CO_2 sequestration at nanoscale interfaces. Chemical Engineering Journal, 2014, 255: 705-715.
Jeon, P. R., Kim, D.-W., Lee, C.-H. Dissolution and reaction in a CO_2-brine-clay mineral particle system under geological CO_2 sequestration from subcritical to supercritical conditions. Chemical Engineering Journal, 2018, 347: 1-11.
Jing, J., Yang, Y., Cheng, J., et al. Analysis of the effect of formation dip angle and injection pressure on the injectivity and migration of CO_2 during storage. Energy, 2023, 280: 128021.
Jung, H. B., Um, W. Experimental study of potential wellbore cement carbonation by various phases of carbon dioxide during geologic carbon sequestration. Applied Geochemistry, 2013, 35: 161-172.
Kim, J., Toshifumi, M., Xue, Z. Monitoring and detecting CO_2 injected into water-saturated sandstone with joint seismic and resistivity measurements. Exploration Geophysics, 2011, 42(1): 58-68.
Kishida, K., Yamauchi, Y., Guzik, A. Study of optical fibers strain-temperature sensitivities using hybrid Brillouin-Rayleigh system. Photonic Sensors, 2014, 4(1): 1-11.
Kroeger, K. F., Jalilinasrabady, S., Sahoo, T. Carbon dioxide plume prediction for site assessment and fault leakage risk in a seismically active region (Taranaki Basin, New Zealand). Geoenergy Science and Engineering, 2025, 254: 214007.
Kutchko, B. G., Strazisar, B. R., Dzombak, D. A., et al. Degradation of well cement by CO_2 under geologic sequestration conditions. Environmental Science & Technology, 2007, 41(13): 4787-4792.
Lian, W., Li, J., Xu, D., et al. Sealing failure mechanism and control method for cement sheath in HPHT gas wells. Energy Reports, 2023, 9: 3593-3603.
Li, D., Jiang, X. Numerical investigation of the partitioning phenomenon of carbon dioxide and multiple impurities in deep saline aquifers. Applied Energy, 2017, 185: 1411-1423.
Linda, S., Chris, B., Jim, U., et al. Application of tracers to measure, monitor and verify breakthrough of sequestered CO_2 at the CO_2CRC Otway project, Victoria, Australia. Chemical Geology, 2014, 399: 2-19.
Li, S., Dong, M., Li, Z., et al. Gas breakthrough pressure for hydrocarbon reservoir seal rocks: Implications for the security of long-term CO_2 storage in the Weyburn field. Geofluids, 2005, 5(4): 326-334.
Li, S., Wang, L., Su, L., et al. Carbon dioxide diffusions in methane-dissolved pore fluids: Implications for geological carbon storage and utilization in tight formations. Chemical Engineering Journal, 2022a, 429: 132147.
Liu, Q., Du, Y., Li, S., et al. Wettability-controlled CO_2 hydrate growth in porous media: Insights from NMR and microfluidic studies. Chemical Engineering Journal, 2026, 529: 172983.
Liu, Q., Zhu, D., Jin, Z., et al. Carbon capture and storage for long-term and safe sealing with constrained natural CO_2 analogs. Renewable and Sustainable Energy Reviews, 2023, 171: 113000.
Liu, T., Li, Q., Li, X., et al. A critical review of distributed fiber optic sensing applied to geologic carbon dioxide storage. Greenhouse Gases: Science and Technology,

2024a, 14(4): 676-694.
Liu, X., Tan, J., Wang, Q., et al. Surface morphologic changes and mineral transformation mechanisms after CO_2-brine-rock reaction in organic matter-rich ferroan shale. Chemical Engineering Journal, 2024b, 498: 155130.
Li, X., Zeng, Y., Muchiri, N. D., et al. The use of distributed acoustic sensing (DAS) in monitoring the integrity of cement-casing system. Journal of Petroleum Science and Engineering, 2022b, 208: 109690.
Li, Y., Wang, Y., Dan, W., et al. CO_2 seepage & breakthrough process and multifactorial influence mechanisms on it in unsaturated low-permeability sandstones. Journal of Hydrology, 2025, 659: 133331.
Li, Z., Yuan, L., Sun, G., et al. Experimental determination of CO_2 diffusion coefficient in a brine-saturated core simulating reservoir condition. Energies, 2021, 14(3): 540.
Lu, S., Hu, C., Wang, X., et al. Carbon dioxide storage in clastic rocks: Review and perspectives. Renewable and Sustainable Energy Reviews, 2025, 213: 115487.
Ma, C., Lin, C., Dong, C., et al. Determination of the critical flow pore diameter of shale caprock. Marine and Petroleum Geology, 2020a, 112: 104042.
Ma, C., Lin, C., Dong, C., et al. Quantitative relationship between argillaceous caprock thickness and maximum sealed hydrocarbon column height. Natural Resources Research, 2020b, 29(3): 2033-2049.
Marapira, T., Alafnan, S., Raza, A., et al. Accelerated CO_2 dissolution and mineralization in saline aquifers using alkaline earth metals. Chemical Engineering Journal, 2025, 523: 168207.
Mehmani, Y., Xu, K. A continuum theory of diffusive bubble depletion in porous media. Advances in Water Resources, 2024, 185: 104625.
Mouallem, J., Arif, M., Isah, A., et al. Effect of formation brine on interfacial interaction: Implications for CO_2 storage. Fuel, 2024, 371: 131986.
Nešić, S. Key issues related to modelling of internal corrosion of oil and gas pipelines-a review. Corrosion Science, 2007, 49(12): 4308-4338.
Norouzi, A. M., Babaei, M., Han, W. S., et al. CO_2-plume geothermal processes: A parametric study of salt precipitation influenced by capillary-driven backflow. Chemical Engineering Journal, 2021, 425: 130031.
Omrani, S., Ghasemi, M., Mahmoodpour, S., et al. Insights from molecular dynamics on CO_2 diffusion coefficient in saline water over a wide range of temperatures, pressures, and salinity: CO_2 geological storage implications. Journal of Molecular Liquids, 2022, 345: 117868.
Padhi, A., Mallick, S., Behzadi, H., et al. Efficient modeling of seismic signature of patchy saturation for time lapse monitoring of carbon sequestrated deep saline reservoirs. Applied Energy, 2014, 114: 445-455.
Peng, H., Xu, Z., Lu, H., et al. Numerical stress and damage analysis of cement plug under casing corrosion in CO_2 geological sequestration. Process Safety and Environmental Protection, 2025, 193: 1036-1049.
Peng, H., Xu, Z., Xia, Z., et al. Closed wellbore integrity failure induced by casing corrosion based on solid-chemical coupling model in CO_2 sequestration. Geoenergy Science and Engineering, 2024, 241: 213140.
Pradhan, S., Bhattacherjee, R., Aichele, C., et al. Determination of CO_2 solubility in brines and produced waters of various salinities for CO_2-EOR and storage applications. Chemical Engineering Journal, 2025, 507: 160401.
Qafoku, N. P., Lawter, A. R., Bacon, D. H., et al. Review of the impacts of leaking CO_2 gas and brine on groundwater quality. Earth-Science Reviews, 2017, 169: 69-84.
Qian, C., Rui, Z., Liu, Y., et al. Microfluidic investigation on microscopic flow and displacement behavior of CO_2 multiphase system for CCUS-EOR in heterogeneous porous media. Chemical Engineering Journal, 2025, 505: 159135.
Qingyun, L., Mook, L. Y., M, F. K., et al. Chemical reactions of portland cement with aqueous CO_2 and their impacts on cement's mechanical properties under geologic CO_2 sequestration conditions. Environmental Science & Technology, 2015, 49(10): 6335-6343.
Qu, A., Liu, M., Huang, Y., et al. Enhancement of the fluid diffusion-dominated mineralization storage in the wet supercritical CO_2 system. Chemical Engineering Journal, 2025, 521: 166547.
Ramadhan, R., Promneewat, K., Thanasaksukthawee, V., et al. Geomechanics contribution to CO_2 storage containment and trapping mechanisms in tight sandstone complexes: A case study on Mae Moh Basin. Science of The Total Environment, 2024, 928: 172326.
Ren, J., Sun, L., Li, X., et al. Interfacial dynamics and mass transfer in underground hydrogen storage applications: A review of H_2 flow, stability and storage performance. Advances in Geo-Energy Research, 2025, 18(2): 121-136.
Rezaeyan, A., Tabatabaei-Nejad, S. A., Khodapanah, E., et al. A laboratory study on capillary sealing efficiency of Iranian shale and anhydrite caprocks. Marine and Petroleum Geology, 2015, 66: 817-828.
Rock, L., Villegas, E. I., Becker, V., et al. Investigation of natural tracers for MMV at the Quest carbon capture and storage project, Alberta, Canada. Energy Procedia, 2014, 63: 4191-4198.
Saraf, S., Bera, A. A review on pore-scale modeling and CT scan technique to characterize the trapped carbon dioxide in impermeable reservoir rocks during sequestration. Renewable and Sustainable Energy Reviews, 2021, 144: 110986.
Sarmadivaleh, M., Al-Yaseri, A. Z., Iglauer, S. Influence of temperature and pressure on quartz-water-CO_2 contact angle and CO_2-water interfacial tension. Journal of Colloid and Interface Science, 2015, 441: 59-64.
Schmidt-Hattenberger, C., Bergmann, P., Labitzke, T., et al. CO_2 migration monitoring by means of electrical resistivity tomography (ERT)-review on five years of operation of a permanent ERT system at the Ketzin Pilot Site. Energy Procedia, 2014, 63: 4366-4373.
Shao, Z., Fang, Z., Sakai, Y. Enhancement of compacted hardened cement paste powder through carbonation: Evo-

lution of CO_2 diffusion, phase assemblage and pore structure. Case Studies in Construction Materials, 2025, 23: e05293.

Shi, M., Xu, J., Wang, X., et al. Understanding of dynamic cement-rock interaction in the wellbore during CO_2 geological storage by using X-ray CT. Construction and Building Materials, 2025a, 484: 141769.

Shi, X., Zhang, C., Gupta, K. K., et al. Risks of cement and rock-cement-metal interface degradation in geological carbon sequestration reservoirs: Mechanisms, influencing factors and mitigation measures. Carbon Capture Science & Technology, 2025b, 15: 100419.

Shumski, A., Diemler, N., Wright, R., et al. TiO_2 coated optical fibers for distributed real-time pH monitoring in wellbore conditions. Paper 12105 Presented at SPIE Defense+Commercial Sensing, Orlando, Florida, United States, 3-7 April, 2022.

Sohal, M. A., Le Gallo, Y., Audigane, P., et al. Effect of geological heterogeneities on reservoir storage capacity and migration of CO_2 plume in a deep saline fractured carbonate aquifer. International Journal of Greenhouse Gas Control, 2021, 108: 103306.

Song, J., Chen, R., Wu, Z., et al. A review of research methods for oil well cement corroded by carbon dioxide. Geoenergy Science and Engineering, 2024a, 232: 212469.

Song, Y., Yao, C., Zhang, X., et al. Experimental investigation on influencing factors of caprock breakthrough pressure under CO_2 geological sequestration. Paper Presented at Progress and Challenge of Porous Media: Proceedings of the 16th Annual Meeting Conference on Porous Media, Singapore, 13-16 May, 2024b.

Stalker, L., Boreham, C., Underschultz, J., et al. Geochemical monitoring at the CO_2CRC Otway project: Tracer injection and reservoir fluid acquisition. Energy Procedia, 2009, 1(1): 2119-2125.

Stavropoulou, E., Laloui, L. Evaluating CO_2 breakthrough in a shaly caprock material: A multi-scale experimental approach. Scientific Reports, 2022, 12(1): 10706.

Stephen, H., Jonathan, H., Henning, K., et al. Quest CCS facility: Time-lapse seismic campaigns. International Journal of Greenhouse Gas Control, 2022, 117: 103665.

Sun, L., Liu, Y., Ren, J., et al. Salt precipitation and pore structure changes during CO_2 injection into porous media. Journal of Cleaner Production, 2025, 505: 145446.

Sun, Y., Yuan, S., Bai, Z., et al. A unique anti-corrosion composite coating with CO_2 gas barrier and acid resistance suitable for CCUS environment. Chemical Engineering Journal, 2023, 472: 144879.

Tan, Y., Li, Q., Xu, L., et al. Investigation of imbibition and strain behavior of longmaxi shale using fiber Bragg grating sensing. Journal of Rock Mechanics and Geotechnical Engineering, 2025, 17(12): 7546-7554.

Topham, A., Lofts, J., Du, Z., et al. 3-Axis borehole gravity: Method and application to CO_2 storage monitoring and oil/gas production. Paper 201441 Presented at SPE Annual Technical Conference and Exhibition, Virtual, 26-29 October, 2020.

Udebhulu, O. D., Aladeitan, Y., Azevedo, R. C., et al. A review of cement sheath integrity evaluation techniques for carbon dioxide storage. Journal of Petroleum Exploration and Production Technology, 2024, 14(1): 1-23.

Wang, D., Li, J., Lian, W., et al. Evolution of cementing properties of wellbore cement under CO_2 geological storage conditions. Construction and Building Materials, 2024a, 452: 138927.

Wang, H., Li, Y., Li, C., et al. Unveil the controls on CO_2 diffusivity in saline brines for geological carbon storage. Geoenergy Science and Engineering, 2025a, 244: 213483.

Wang, H., Zhang, L., Gan, M., et al. Temperature and reaction time's effects on N80 steel corrosion behavior in supercritical CO_2 and formation water environments. Applied Sciences, 2024b, 14(2): 728.

Wang, W., Liang, Z., Li, Y., et al. Metal mobilization and pore alterations during CO_2 storage in the Yanchang formation tight sandstone, Ordos Basin. Chemical Engineering Journal, 2025b, 507: 160874.

Wang, Z., Sun, Y., Kong, H., et al. An in-depth review of key technologies and pathways to carbon neutrality: Classification and assessment of decarbonization technologies. Carbon Neutrality, 2025c, 4(1): 15.

Wei, L., Pang, X., Liu, C., et al. Formation mechanism and protective property of corrosion product scale on X70 steel under supercritical CO_2 environment. Corrosion Science, 2015, 100: 404-420.

Wei, N., Li, X., Wang, Y., et al. Experimental studies of CO_2 breakthrough pressure of argillaceous siltstone under different pressures and temperatures. Rock and Soil Mechanics, 2014, 35(1): 98-104. (in Chinese)

Welch, N. J., Frash, L. P., Harp, D. H., et al. Shear strength and permeability of the cement-casing interface. International Journal of Greenhouse Gas Control, 2020, 95: 102977.

White, J. C., Williams, G., Chadwick, A., et al. Sleipner: The ongoing challenge to determine the thickness of a thin CO_2 layer. International Journal of Greenhouse Gas Control, 2018, 69: 81-95.

Wollenweber, J., Alles, S., Busch, A., et al. Experimental investigation of the CO_2 sealing efficiency of caprocks. International Journal of Greenhouse Gas Control, 2010, 4(2): 231-241.

Wolterbeek, T. K. T., Peach, C. J., Spiers, C. J. Reaction and transport in wellbore interfaces under CO_2 storage conditions: Experiments simulating debonded cement-casing interfaces. International Journal of Greenhouse Gas Control, 2013, 19: 519-529.

Xia, Y., Xu, T., Yang, Z., et al. Factors influencing amount of CO_2 leakage through a fault zone in deep storage aquifer. Research of Environmental Sciences, 2017, 30(10): 1533-1541. (in Chinese)

Xue, Q., Zhang, L., Mei, K., et al. Evolution of structural and mechanical properties of concrete exposed to high concentration CO_2. Construction and Building Materials, 2022, 343: 128077.

Xu, J., Li, C., Shi, M., et al. Monitoring fluid migration in a CO_2 storage reservoir by distributed fiber optic strain sensing: A laboratory study. Gas Science and

Engineering, 2024, 124: 205270.
Xu, L., Li, Q., Tan, Y., et al. Characterization of carbon dioxide leakage process along faults in the laboratory. Journal of Rock Mechanics and Geotechnical Engineering, 2022, 14(3): 674-688.
Yang, F., Okwen, R. Determining the brine extraction well type, location, and rate for optimal pressure and carbon dioxide plume management. Gas Science and Engineering, 2024, 121: 205174.
Yang, K., Zhou, J., Xian, X., et al. Changes of wettability of shale exposed to supercritical CO_2-water and its alteration mechanism: Implication for CO_2 geo-sequestration. Fuel, 2024a, 357: 129942.
Yan, W., Sinan, L., Liwei, Z., et al. Evidence of self-sealing in wellbore cement under geologic CO_2 storage conditions by micro-computed tomography (CT), scanning electron microscopy (SEM) and Raman observations. Applied Geochemistry, 2021, 128: 104937.
Yan, W., Wei, H., Muchiri, N. D., et al. Degradation of chemical and mechanical properties of cements with different formulations in CO_2-containing HTHP downhole environment. Petroleum Science, 2023, 20(2): 1119-1128.
Yao, C., Zhang, X., Song, Y., et al. Experimental investigation of fractured caprock breakthrough pressure under different proportions of sequestered gas conditions. Paper Presented at Progress and Challenge of Porous Media: Proceedings of the 16th Annual Meeting Conference on Porous Media, Singapore, 13-16 May, 2025.
Yu, W., Lo, J. H. Y., Adebayo, A. R., et al. Microfluidic study of CO_2 diffusive leakage through microfractures in saline aquifers for CO_2 sequestration. Advances in Water Resources, 2025, 200: 104960.
Zhang, D., Wang, F., Li, Q., et al. Study on early seal failure of CO_2-injected packer based on orthogonal experimental method. Alexandria Engineering Journal, 2023a, 72: 695-707.
Zhang, L., Zhang, S., Shan, L., et al. A comprehensive analysis to illustrate complex migration behaviors of fluid along fault for CO_2 geological storage. Energy, 2025, 334: 137673.
Zhang, W., Wu, S., Ren, S., et al. The modeling and experimental studies on the diffusion coefficient of CO_2 in saline water. Journal of CO_2 Utilization, 2015, 11: 49-53.
Zhang, Y., Geng, W., Chen, M., et al. Experimental measurements of the diffusion coefficient and effective diffusion coefficient of CO_2-brine under offshore CO_2 storage conditions. Energy & Fuels, 2023b, 37(24): 19695-19703.
Zhang, Y., Liu, Y., Lv, Q., et al. Time-lapse gravity monitoring technology and prospects for carbon dioxide geological storage. Progress in Geophysics, 2024, 40(2): 495-510. (in Chinese)
Zhang, Y., Xue, Z. Deformation-based monitoring of water migration in rocks using distributed fiber optic strain sensing: A laboratory study. Water Resources Research, 2019, 55(11): 8368-8383.
Zhang, Y., Xue, Z., Park, H., et al. Tracking CO_2 plumes in clay-rich rock by distributed fiber optic strain sensing (DFOSS): A laboratory demonstration. Water Resources Research, 2019, 55(1): 856-867.
Zheng, W., Lu, X., Zhang, X., et al. The effect of caprock permeability on the leakage of CO_2 in a CO_2 capture and storage project. Mechanics in Engineering, 2010, 32(4): 30-34. (in Chinese)
Zhong, Y., Song, J., Wang, X., et al. Improvement of the resistance to carbon dioxide corrosion of oil well cement by micron diabase powder in high-temperature environment. Construction and Building Materials, 2024, 452: 138884.
Zhou, N., Wu, L., Yuan, J., et al. Feasibility evaluation of cement sheath sealing within large-size casing structures in gas and hydrogen storage wells. International Journal of Hydrogen Energy, 2025, 115: 265-280.
Zhu, Y., He, Z., Wang, H., et al. CO_2 leakage in geologic carbon storage: A review of its impacts and detection. Chemical Engineering Journal, 2025, 523: 168423.